MUTUAL IMPEDANCE CONSIDERATIONS IN TWO DIMENSIONAL PLANAR ACOUSTIC ARRAYS WITH SQUARE PISTON ELEMENTS

A THESIS SUBMITTED TO

THE GRADUATE SCHOOL OF ENGINEERING AND SCIENCE

OF BILKENT UNIVERSITY

IN PARTIAL FULFILLMENT OF THE REQUIREMENTS FOR

THE DEGREE OF

MASTER OF SCIENCE

IN

ELECTRICAL AND ELECTRONICS ENGINEERING

By

Mustafa Oğuzhan Saçma

December, 2015

MUTUAL IMPEDANCE CONSIDERATIONS IN TWO DIMENSIONAL PLANAR ACOUSTIC ARRAYS WITH SQUARE PISTON ELEMENTS
By Mustafa Oğuzhan Saçma
December, 2015

We certify that we have read this thesis and that in our opinion it is fully adequate, in scope and in quality, as a thesis for the degree of Master of Science.

Hayrettin Köymen(Advisor)

Ayhan Altıntaş

Arif Sanlı Ergün

Approved for the Graduate School of Engineering and Science:

Levent Onural
Director of the Graduate School

ABSTRACT

MUTUAL IMPEDANCE CONSIDERATIONS IN TWO DIMENSIONAL PLANAR ACOUSTIC ARRAYS WITH SQUARE PISTON ELEMENTS

Mustafa Oğuzhan Saçma
M.S. in Electrical and Electronics Engineering
Advisor: Hayrettin Köymen
December, 2015

Large acoustic arrays have tremendous value in military and civil applications for producing well-formed beams. In order to realize the potential gains of these applications enabled by large acoustic arrays, it is essential to calculate and take into account the acoustic coupling of the sonar arrays. Although many studies have been conducted on this phenomenon, the practical and theoretical studies in public literature remain inadequate especially on mutual radiation impedance of the acoustic sonar arrays. In order to address this need, self and mutual radiation impedances of square piston elements in two-dimensional planar acoustic arrays are investigated in this thesis. Impedance matrices are formed from the self and mutual radiation impedances of these elements. Operation of arrays and possible mutual radiation impedances are analyzed through the active simulations of planar arrays. Importantly, the mutual impedance data is tested on a generic equivalent circuit model of a piston transducer. Resonance of these transducers and Rayleigh-Bloch waves are also observed as the outcome of these tests.

Keywords: Mutual Acoustic Coupling, Self and Mutual Radiation Impedances, Planar Array, Square Piston Elements, Transducer, Rayleigh-Bloch Waves.

ÖZET

İKİ BOYUTLU DÜZLEMSEL AKUSTİK DİZİNLERDE KARE PİSTON ELEMANLAR İÇİN KARŞILIKLI EMPEDANS DEĞERLENDİRMELERİ

Mustafa Oğuzhan Saçma
Elektrik ve Elektronik Mühendisliği, Yüksek Lisans
Tez Danışmanı: Hayrettin Köymen
Aralık, 2015

Büyük akustik dizinler, askeri ve sivil uygulamalarda iyi oluşturulmuş hüzme oluşturabilmek için yüksek öneme sahiptir. Bu uygulamaların olası kazançlarını elde edebilmek için sonar dizinlerindeki akustik eşlenimi dikkate almak ve hesaplamak gereklidir. Bu konu üzerinde çok sayıda çalışma yapılmış olmasına rağmen, özellikle kare piston elemanların karşılıklı radyasyon empedansıyla ilgili teorik ve pratik olarak yayınlanmış akademik yazınlar yetersizdir. Bu eksiği gidermek adına, bu tezde iki boyutlu düzlemsel dizinlerdeki kare piston transdüserlerin öz ve karşılıklı radyasyon empedans değerleri incelenmektedir. Bu elemanların öz ve karşılıklı radyasyon empedans değerleri ile empedans matrisleri oluşturulmaktadır. Ayrıca, dizinlerin çalışması ve olası radyasyon empedans değerleri aktif simülasyonlar ile analiz edilmiştir. Karşılıklı empedans verileri, transdüserlerin jenerik eşdeğer devre modeli ile test edilerek farklı parametrelerde rezonansları incelenmiş ve Rayleigh-Bloch dalgaları gözlemlenmiştir.

Anahtar sözcükler: Karşılıklı Akustik Bağlaşım, Öz ve Karşılıklı Radyasyon Empedansları, Düzlemsel Dizin, Kare Piston Elemanlar, Transdüser, Rayleigh-Bloch Dalgaları.

Acknowledgement

First and foremost, I would like to express my deepest gratitude to my supervisor Professor Hayrettin Köymen, for his guidance and the opportunity to study in this research field. It has been a privilege to work under his supervision. I owe my sincerest gratitude to him for his continuous support and belief during my graduate studies. He has supported and encouraged me since I started my undergraduate education.

I also thank Prof. Ayhan Altıntaş and Assoc. Prof. Arif Sanlı Ergün for reviewing my thesis and their contributions. Their comments and support are very much appreciated.

I would like to give my special thanks to my colleagues Dr. H. Kağan Oğuz, Dr. Alper Bereketli, M. Talha Işık and M. Ertuğ Olgun. It would not have been possible to conduct this research without their support and motivation.

I also would like to show gratitude to my friends Bahadır, Cengiz, Gözde, Özgür Öner, and Emre, who were always helping and encouraging me.

The work presented in the thesis would not have been possible without the advice, guidance, and help from many people. A very special thanks to my mother Gülşen, my sister Aslıhan and my father Muhammet for their trust and endless love.

Finally, I would like to acknowledge the financial support from TÜBİTAK BİDEB 2210 Program.

Contents

List of Figures

Chapter 1

Introduction

Sound is the mechanical wave of pressure and displacement as a propagation of vibration through a medium. The interdisciplinary science that focuses on this subject is acoustics. In acoustics, sound is the core element for many applications. Sonar (sound navigation and ranging) systems that use sound propagation for navigating, detecting friend/foes and communication purposes is an important part of this study area. For instance, in naval applications, searching for other ships/submarines and sustaining underwater communication are crucial functions that sonar has to accomplish. Development of large projector arrays is important when it is necessary to work with innovative sonar systems. A wide range of operations requires the employment of projector arrays. They operate in the 2-10 kHz region for medium range performance for active search and they use higher frequencies for smaller objects, while in some cases they need to bare hydrostatic pressure with stable results. Long-range sonar systems need lower frequency and higher power for efficient detection.

Arrays in general may contain hundreds of transducers, depending on the objective of the system. These transducers are usually placed on spherical, cylindrical or plane surface and connected to the ports of the main system. In order to maximize acoustic power and have well-defined beam forming, transducers are mounted next to each other. On the other hand, the placement of transducers has influence on each other through acoustic coupling. Thus, each transducer vibrates due to the vibration of other transducers in addition to the intrinsic vibration caused by its electrical input. Acoustic coupling directly affects the performance of the array. These effects must be estimated by considering the mutual radiation impedance relations in array design process.

The array design focuses on acoustic performance. The data such as maximum acoustic power, maximum source level, beam width and directivity index (DI) of the output signal determine the characteristics. However, the design is incomplete without including the effect of acoustic coupling, since the power of transducers and their working regime change significantly due to the acoustic coupling.

In this work, the acoustic coupling between the array elements is studied and emphasis is placed on piston transducers. In sonar arrays, elements affect each other's performance due to the mutual radiation impedance effects. These effects can be interpreted as pressure on each element, which is generated by the particle velocity of the other elements. It is important to know and consider these effects in array design since these effects can change the beam forming and the pressure levels. They can even lead to the destruction of array elements [1]. A common piston shape in arrays is the circular piston. The flexible circular pistons had been popular array elements after progress in CMUT (Capacitive Micromachined Ultrasonic Transducers) technology [2, 3]. For the crosstalk issues, there exists a significant body of research on mutual radiation impedance effects in CMUT arrays [4, 5, 6, 7, 8]. Flexible circular pistons differ from circular pistons due to the particle velocity profile on the surface and, hence, the self and mutual radiation impedance.

On the other hand, this thesis focuses on a more basic piston type, square piston. The basis of the theory on square pistons has been studied previously. Upon these studies, self-radiation impedance of a rigid square piston in an infinite baffle has been calculated [9]. Mutual radiation impedance of rectangular and circular pistons is also studied [10, 11, 12, 13, 14, 15, 16, 17, 18, 19, 20, 21]. Transducers on a cylinder or a sphere also exhibit these acoustic coupling phenomena [22, 23]. Although there is a solid basic information and research, the available knowledge on square pistons remains inadequate. In this study, we shall consider arrays of square piston transducers. Since, the self and mutual radiation impedance of square pistons is different from circular pistons and any others. Thus, constraints on arrays must be developed independently.

This thesis is organized in six chapters. In Chapter 2, we present a review of the array and transducer concepts. Self and mutual radiation impedances are described in Chapter 3 and radiation impedance calculations are also presented. In Chapter 4, we characterize the mutual impedance effects of two-dimensional planar acoustic arrays. Performance evaluation results of a generic equivalent circuit model, which includes the mutual radiation impedance between array elements, are presented in Chapter 5. Finally, the thesis is concluded in Chapter 6.

Chapter 2

Modeling of Arrays

2.1 Arrays and Mutual Impedance

In underwater acoustics, it is common practice to employ sensors in an array formation. In order to have powerful systems and get high performance, individual elements are joined together and they work in synchrony. The elements of array are often piston transducers. Each element is located closely or side-by-side to each other. Size of the array is directly related to the capacity that is demanded from the system. Generally, in order to have a beam-formed signal, there are many elements on an array. For efficient results, the user of the system intends to operate them simultaneously. However, this simultaneous operation could cause adverse effects that have the potential to change the expected process, for instance, beam forming distortion.

In this thesis, we work on square elements due to their wide range of applications. Using this shape, the geometry of the array is suitable to tessellate, since the baffle shall be tiled up eventually. In Fig. 2.1, each element is depicted as a square. In order to emphasize the distance relations between elements, the location of each element is defined as the left-bottom point of each cell as "Location Point". The side length of an element is shown by a, and the distance between

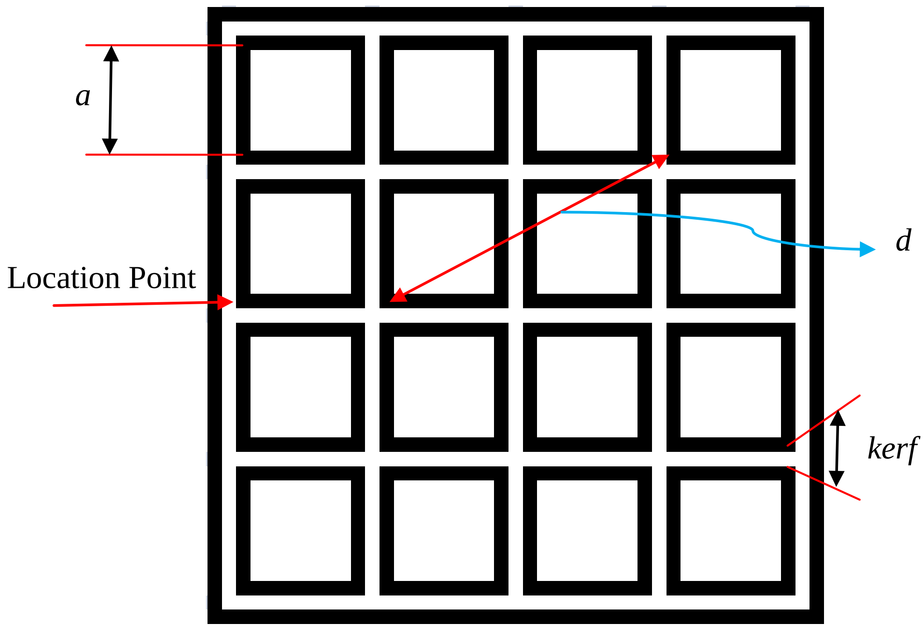

Figure 2.1: Square array

two elements is denoted by d, which is measured from each element's location point. The empty space between the sides of adjacent elements is called $kerf$. Theoretical assumptions, calculations and simulations shall be done by assuming the $kerf$ value is zero. However, it must be taken into account in practice.

2.2 Rigid Baffle

Elements build up the array and that is contained in a rigid baffle. Rigid baffle stands for an infinite baffle surface in contact with the medium such as water. On this surface of the array, vertical component of particle velocity is zero. In order to find impedances and diffractions in a rigid baffle, it is sufficient to assume a particle velocity across the element surface and to carry out the integration only across the element surface area, since particle velocity is zero elsewhere [24].

There is a certain particle velocity across the element surface. Except the effect of this assumption, everything is well known for rigid baffle arrays. Using this assumption, modeling becomes easier, since the surface is driven by a velocity source and complies with the rigid baffle. However, for mechanical ports of transducers, velocity sources are not enough and those ports have impedances, too.

Therefore, the element impedances of the array need to be revised. First, we need to introduce transducer equivalent circuits. In Fig. 2.2, a generic two port equivalent circuit of a transducer, and its transmitting and receiving equivalent circuits are demonstrated [24]. The transducer is powered up from its electrical port. Then, vibration occurs at the mechanical port of the transducer. The force (F) and the particle velocity (U) is the outcome of this operation on the water base where the pressure sourced by this force is valid for all elements of the array as in Fig. 2.3.

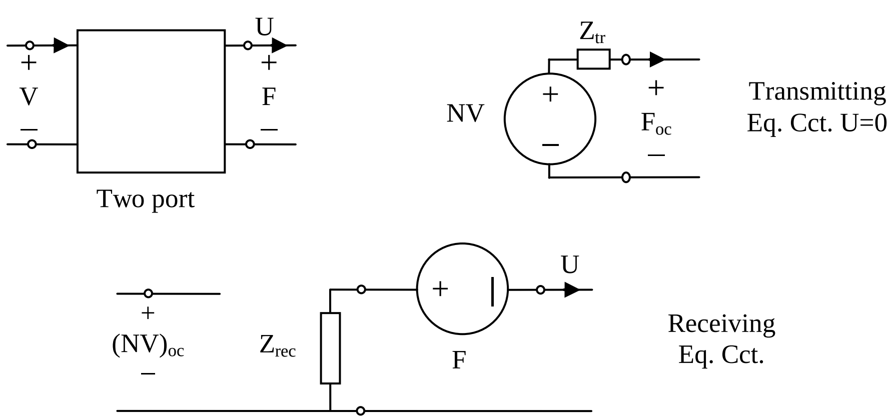

Figure 2.2: Two-port equivalent circuit of a single element transducer

After getting the single element model, we also need to consider the element port placement at the mechanical port interface plane of that array. We assume that we have random square array of i-elements such as Fig. 2.3. For this array, element circuits on the transducer base of the port plane and radiation impedances on the water base of the plane are needed.

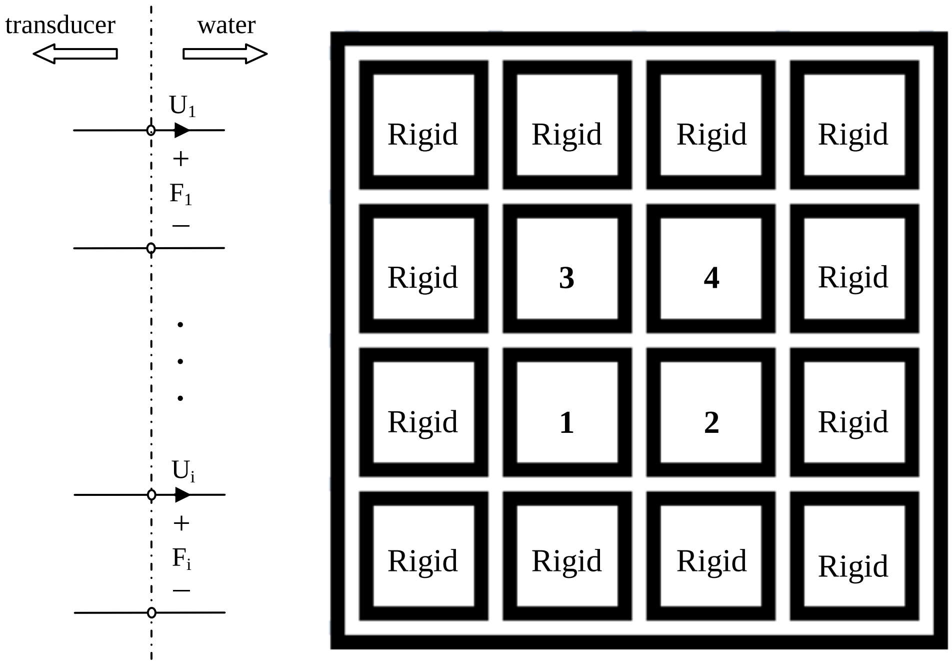

Figure 2.3: Transducer and water base of the plane

Eq. (2.1) demonstrates the impedance relation on the radiation side, semi-infinite space in water, in which the matrix elements are well known.

$$\begin{bmatrix} F_1 \\ F_2 \\ \vdots \\ F_i \end{bmatrix} = \begin{bmatrix} Z_{11} & Z_{12} & \cdots & Z_{1i} \\ Z_{21} & Z_{22} & \cdots & Z_{2i} \\ \vdots & \vdots & \ddots & \vdots \\ Z_{i1} & Z_{i2} & \cdots & Z_{ii} \end{bmatrix} \begin{bmatrix} U_1 \\ U_2 \\ \vdots \\ U_i \end{bmatrix} \tag{2.1}$$

The equations for single element of the transmitting array become Eq. (2.2), after combining the two circuits

$$F_1 = Z_{11}U_1 + \begin{bmatrix} Z_{12} & Z_{13} & \cdots & Z_{1i} \end{bmatrix} \begin{bmatrix} U_2 \\ U_3 \\ \vdots \\ U_i \end{bmatrix} \tag{2.2}$$

$$\text{and} \quad F_1 = N_1V_1 - Z_{tr1}U_1$$

where F_1 is depicted for the water base and the transducer base, respectively.

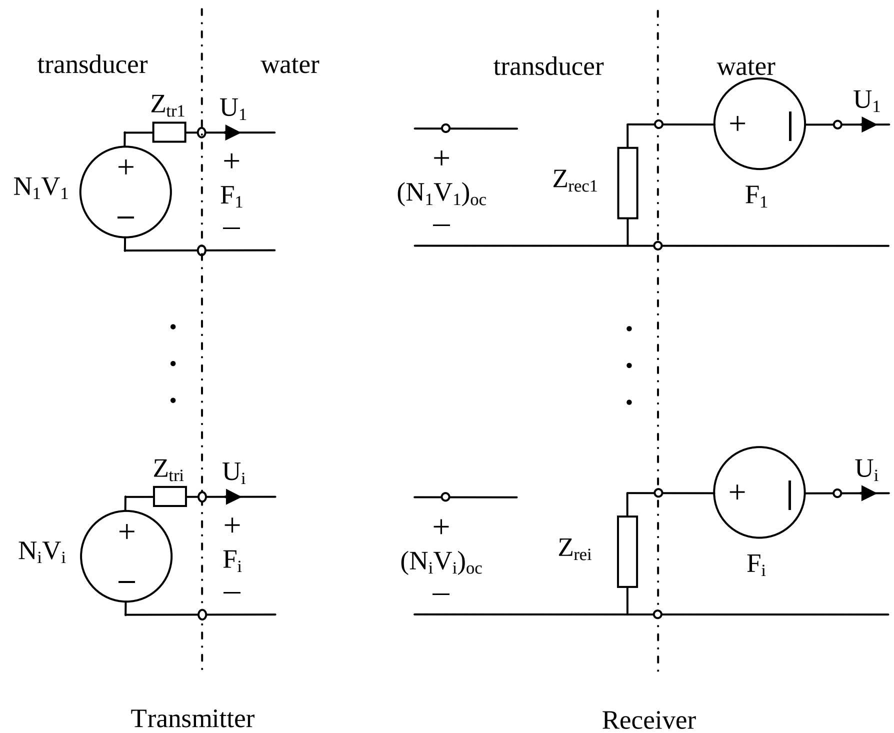

Figure 2.4: Transducer and water base transmitting models

In Fig. 2.4, there are demonstrations to drive the equivalent circuits [24]. Thus, transmitting and receiving is possible. The relation between driving voltage and the mechanical port can be represented with Eq. (2.3):

$$N_1V_1 = Z_{tr1}U_1 + Z_{11}U_1 + \begin{bmatrix} Z_{12} & Z_{13} & \cdots & Z_{1i} \end{bmatrix} \begin{bmatrix} U_2 \\ U_3 \\ \vdots \\ U_i \end{bmatrix} \tag{2.3}$$

After generalizing Eq. (2.3) for the whole ports, we obtain Eq. (2.4) as follows:

$$\begin{bmatrix} N_1V_1 \\ N_2V_2 \\ \vdots \\ N_iV_i \end{bmatrix} = \begin{bmatrix} Z_{tr1}+Z_{11} & Z_{12} & \cdots & Z_{1i} \\ Z_{21} & Z_{tr2}+Z_{22} & \cdots & Z_{2i} \\ \vdots & \vdots & \ddots & \vdots \\ Z_{i1} & \cdots & \cdots & Z_{tri}+Z_{ii} \end{bmatrix} \begin{bmatrix} U_1 \\ U_2 \\ \vdots \\ U_i \end{bmatrix} \tag{2.4}$$

Here, the diagonal entries of the matrix are augmented and they are self-radiation impedances of the elements. For receiver mode, port equations similarly become as Eq. (2.5):

$$\begin{gathered} \begin{bmatrix} F_1 \\ F_2 \\ \vdots \\ F_i \end{bmatrix} = \begin{bmatrix} Z_{rec1}+Z_{11} & Z_{12} & \cdots & Z_{1i} \\ Z_{21} & Z_{rec2}+Z_{22} & \cdots & Z_{2i} \\ \vdots & \vdots & \ddots & \vdots \\ Z_{i1} & \cdots & \cdots & Z_{reci}+Z_{ii} \end{bmatrix} \begin{bmatrix} U_1 \\ U_2 \\ \vdots \\ U_i \end{bmatrix} \\ \text{and} \begin{bmatrix} (N_1V_1)_{oc} \\ (N_2V_2)_{oc} \\ \vdots \\ (N_iV_i)_{oc} \end{bmatrix} = \begin{bmatrix} H_1 & 0 & \cdots & 0 \\ 0 & H_2 & \cdots & 0 \\ \vdots & \vdots & \ddots & \vdots \\ 0 & 0 & \cdots & H_i \end{bmatrix} \begin{bmatrix} U_1 \\ U_2 \\ \vdots \\ U_i \end{bmatrix} \end{gathered} \tag{2.5}$$

Therefore,

$$\begin{gathered} \begin{bmatrix} (N_1V_1)_{oc} \\ (N_2V_2)_{oc} \\ \vdots \\ (N_iV_i)_{oc} \end{bmatrix} = \begin{bmatrix} H_1 & 0 & \cdots & 0 \\ 0 & H_2 & \cdots & 0 \\ \vdots & \vdots & \ddots & \vdots \\ 0 & 0 & \cdots & H_i \end{bmatrix} \\ \times \begin{bmatrix} Z_{rec1}+Z_{11} & Z_{12} & \cdots & Z_{1i} \\ Z_{21} & Z_{rec2}+Z_{22} & \cdots & Z_{2i} \\ \vdots & \vdots & \ddots & \vdots \\ Z_{i1} & \cdots & \cdots & Z_{reci}+Z_{ii} \end{bmatrix}^{-1} \begin{bmatrix} F_1 \\ F_2 \\ \vdots \\ F_i \end{bmatrix} \end{gathered} \tag{2.6}$$

'Rigid baffle' assumption of the array and its surrounding area need further corrections. Those modifications for the transducer impedances are accomplished through corresponding calculations [24]. It is important to note that, this result is accurate as long as the rigid baffle assumption is valid.

These matrices are results of the two port equivalent circuit of the transducer. Transducer's one side is electrical base and the other is water base. At the water base, radiation matrix elements are well known (Eq. (2.1)) and for one element, for instance F_1, combining water base with the transducer base results as Eq. (2.2). When we consider the transmission, mutual impedance elements of the matrix does not change, but for the self-radiation impedance case, we also multiply U_1 with self-transmission impedance of the transmitting equivalent circuit model. Therefore, we have Eq. (2.4). Similarly, reception case is defined also with these matrices. This time, the common points of both sides are particle velocities on the surface. From that point, we can combine two sides and get Eq. (2.6).

Chapter 3

Self and Mutual Impedance

3.1 Self Impedance

Acoustic coupling of the array elements result in mutual impedance. However, modeling an element starts from considering the self-radiation impedance of that particular piston. The self-radiation impedance of an element is well known and commonly used in the design of any acoustic system [9].

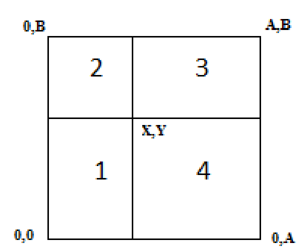

Figure 3.1: Integration area for the self-radiation impedance

Consider a square piston, which is mounted in an infinite rigid plane baffle. To compute its self-radiation impedance we must evaluate the quadruple integral

$$I = \int_0^a \int_0^a \int_0^a \int_0^a \frac{1}{r}\, e^{-jkr} dx dy dX dY \tag{3.1}$$

in Eq. (3.1), where $r = [(x - X)^2 + (y - Y)^2]^{1/2}$ and side length of the piston is a [9]. Fig. 3.1 depicts the integration for the self-radiation impedance of a transducer. For the first two integrations, since (X,Y) is fixed, the whole integral can be divided as in Eq. (3.2),

$$\begin{aligned}\int_0^a \int_0^a f(r) dx dy = \iint_{(1)} f(r) dx dy + \iint_{(2)} f(r) dx dy \\ + \iint_{(3)} f(r) dx dy + \iint_{(4)} f(r) dx dy\end{aligned} \tag{3.2}$$

where $f(r) = \frac{1}{r}\, e^{(-jkr)} dx dy dX dY$ is replaced as the integrand from Eq. (3.1) and (1), (2), (3), (4) are integrations areas which are shown in Fig. 3.1. Integrating the right-hand side of the Eq. (3.2), those four integrals are equal with respect to X and Y. Therefore, we have Eq. (3.3):

$$I = 4 \int_0^a \int_0^a \left[\iint_{(1)} \frac{1}{r}\, e^{-jkr} dx dy \right] dX dY \tag{3.3}$$

One option for calculating this integral is using infinite series. The results are shown below, where they are separated into real and imaginary parts and each part is multiplied by k, which is the wavenumber in the medium [9].

$$Re(kI) = 4k\sum_{n=0}^{\infty} A_{2n}k^{2n}/(2n+2)!$$
$$Im(kI) = -4k^2\sum_{n=0}^{\infty} B_{2n}k^{2n}/(2n+3)!$$

and,

$$A_{2n} = 2(-1)^n a^{2n+3}\left\{\int_0^{\pi/4} sec^{2n+1}\theta d\theta - \frac{2^{n+\frac{1}{2}}-1}{2n+3}\right\}$$
$$B_{2n} = 2(-1)^n a^{2n+4}\left\{\int_0^{\pi/4} sec^{2n+2}\theta d\theta - \frac{2^{n+1}-1}{2n+4}\right\} \tag{3.4}$$

These results of the Eq. (3.4) are multiplied by $j\rho c/2\pi$ and then we obtain self-radiation impedance, where mean density of the fluid medium is ρ and the velocity of phase propagation is c for a given value of ka.

Calculating the self-radiation impedance of a square element with this method is straightforward. Obtained equations are implemented in Matlab software program [25]. A_{2n}, B_{2n} and the other integrals are evaluated numerically. Then, Fig. 3.2 is plotted as the outcome of the implemented code. The integral is separated into its real and imaginary parts. Computation of the integrals is done in the region of every element. The blue line in Fig. 3.2 is the self-radiation resistance as the real part of the impedance, which starts from zero and climbs up to one. Indeed, it oscillates around one, but it converges in specific time as expected. The red line is self-radiation reactance as the imaginary part of the impedance, which again starts from zero. However, for $ka > 3$, reactance starts to decrease and in higher values of ka it is expected to be zero as there cannot be any reactive elements of the impedance at infinity.

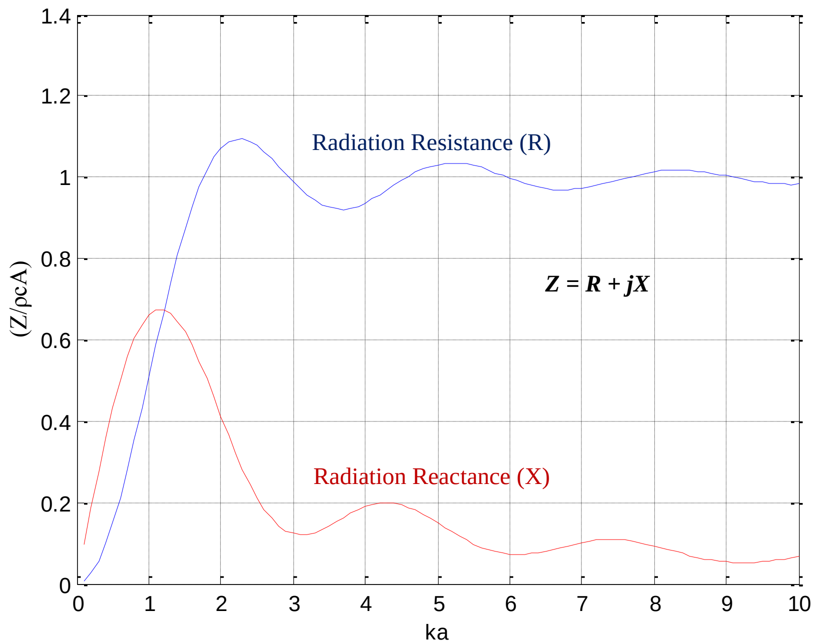

Figure 3.2: Self-radiation impedance ($Z/\rho cA$) of a square element with element dimension ka

3.2 Mutual Impedance

The diagonal entries of the mutual impedance matrix, which are defined in the previous section, are obtained from self-radiation impedance of each element. For all other entries, we need to calculate the mutual radiation impedance between elements, which is also well known and this needs to be implemented in any array design [10]. Therefore, beam forming of that array works efficiently in real operation of acoustic devices.

In the theory for mutual impedance of two elements, the calculations are made for two similar rectangular pistons with side lengths a and b in an infinite rigid plane as shown in Fig. 3.3, where $d = \sqrt{(h^2 + g^2)}$ is the distance between elements and $tan\ \theta = g/h$ is the orientation angle [10]. Rectangular Piston 1 vibrates with angular frequency w and maximum velocity u_0, where the velocity

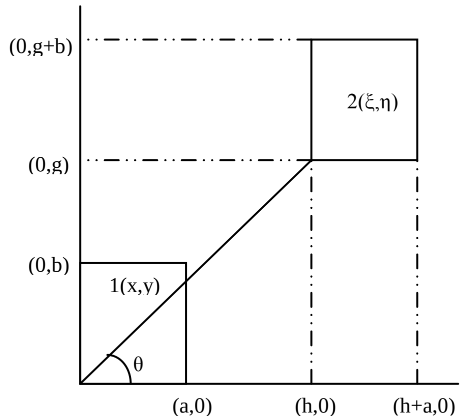

Figure 3.3: Element arrangements and dimensions for mutual radiation impedance as a and b are side lengths and g and h are distance parameters

of sound in the medium is c, the density is ρ, and the wavenumber is k.

$$p = -\frac{j\rho cku_0}{2\pi}e^{-jwt}\int_{x=0}^{a}\int_{x=0}^{b}\frac{e^{jk[(\xi-x)^2+(y-\eta)^2]^{\frac{1}{2}}}}{[(\xi-x)^2+(y-\eta)^2]^{\frac{1}{2}}}dxdy \tag{3.5}$$

This causes a pressure at a point $P(\xi,\eta)$ on Piston 2 as in Eq. (3.5). Motion of Piston 1 on Piston 2 produces a force. Dividing it by the velocity of Piston 1 gives the mutual radiation impedance of the pistons, this can be written as in Eq. (3.6) [10].

$$\begin{gathered} Z_m = -\frac{j\rho ck}{2\pi}\int_0^a\int_0^b\int_h^{h+a}\int_g^{g+b}\frac{e^{jk[(\xi-x)^2+(y-\eta)^2]^{\frac{1}{2}}}}{[(\xi-x)^2+(y-\eta)^2]^{\frac{1}{2}}}dxdyd\xi d\eta \\ Z_m = -\frac{j\rho ck}{2\pi}G_m \end{gathered} \tag{3.6}$$

G_m can be divided into parts as in Eq. (3.7) after the integration:

$$
\begin{aligned}
G_m = & \int_{h-a}^{h} \int_{g-b}^{g} (u+a-h)(v+b-g) \frac{e^{jk[u^2+v^2]^{\frac{1}{2}}}}{[u^2+v^2]^{\frac{1}{2}}} dudv \\
& + \int_{h}^{h+a} \int_{g-b}^{g} (a+h-u)(v+b-g) \frac{e^{jk[u^2+v^2]^{\frac{1}{2}}}}{[u^2+v^2]^{\frac{1}{2}}} dudv \\
& + \int_{h-a}^{h} \int_{g}^{g+b} (u+a-h)(b+g-v) \frac{e^{jk[u^2+v^2]^{\frac{1}{2}}}}{[u^2+v^2]^{\frac{1}{2}}} dudv \\
& + \int_{h}^{h+a} \int_{g}^{g+b} (a+h-u)(b+g-v) \frac{e^{jk[u^2+v^2]^{\frac{1}{2}}}}{[u^2+v^2]^{\frac{1}{2}}} dudv
\end{aligned}
\tag{3.7}
$$

The following coordinate transformation is used for evaluating the G_m integral,

$$
u' = x + \xi, \qquad u = x - \xi, \qquad v' = y + \eta, \qquad v = y - \eta, \tag{3.8}
$$

as $-u + 2h \leq u' \leq u + 2a$ for $h - a \leq u \leq h$ and $u \leq u' \leq 2(h+a) - u$ for $h \leq u \leq h + a$, and identical limits for v also apply [10].

G_m includes $\iint uv \frac{e^{jk[u^2+v^2]^{\frac{1}{2}}}}{[u^2+v^2]^{\frac{1}{2}}} dudv$ type integrals, which are evaluated directly. Other integrations of Eq. (3.6) have a form, where the lower limits are zero:

$$
\begin{aligned}
& \int_0^x \int_0^y (xy - yu - xv) \frac{e^{jk[u^2+v^2]^{\frac{1}{2}}}}{[u^2+v^2]^{\frac{1}{2}}} dudv \\
& = \left(\frac{j}{k}\right) \Bigg\{ y \int_x^{[x^2+y^2]^{\frac{1}{2}}} \frac{e^{jkr}}{r} [r^2 - x^2]^{\frac{1}{2}} dr \\
& \quad + x \int_y^{[x^2+y^2]^{\frac{1}{2}}} \frac{e^{jkr}}{r} [r^2 - y^2]^{\frac{1}{2}} dr \Bigg\} \\
& \quad + \frac{x+y}{k^2} - \frac{y e^{jky}}{k^2} - \frac{x e^{jkx}}{k^2} + \frac{jxy}{k} \frac{\pi}{2}
\end{aligned}
\tag{3.9}
$$

Here, $\int_0^x \int_0^y xy \frac{e^{jk[u^2+v^2]^{\frac{1}{2}}}}{[u^2+v^2]^{\frac{1}{2}}} dudv$ type of integrations can be calculated with a method of changing polar coordinates and then using separated integration regions. The rest has been integrated, and Eq. (3.9) is acquired after combining the same upper and lower limits [10]. In this particular calculations, general case is assumed, where $g \neq 0, h \neq 0$. Then, we obtain G_m as in Eq. (3.10):

$$\begin{aligned} G_m = 4B(h,g) - 2B(h-a,g) - 2B(h,g-b) - 2B(h,g+b) \\ -2B(h+a,g) + B(h-a,g+b) + B(h-a,g-b) \\ + B(h+a,g-b) + B(h+a,g+b) \text{ for } g \neq 0, h \neq 0 \end{aligned} \tag{3.10}$$

where, $B(x,y)$ function is given as Eq. (3.11) [10].

$$\begin{aligned} B(x,y) = \frac{j}{k^3} e^{jk(u^2+v^2)^{\frac{1}{2}}} \{jk(u^2+v^2)^{\frac{1}{2}} - 1\} \\ + \frac{j|x|}{k} \int_{|y|}^{(x^2+y^2)^{\frac{1}{2}}} \frac{e^{jkr}}{r} (r^2 - y^2)^{\frac{1}{2}} dr \\ + \frac{j|y|}{k} \int_{|x|}^{(x^2+y^2)^{\frac{1}{2}}} \frac{e^{jkr}}{r} (r^2 - x^2)^{\frac{1}{2}} dr \end{aligned} \tag{3.11}$$

Mutual radiation impedance, Z_m, can be separated into real and imaginary parts such as $Z_m = R_m + jX_m$, where R_m is the mutual radiation resistance and X_m is the mutual radiation reactance. Mutual radiation resistance becomes as Eq. (3.12) with the following notation: $A = ab, ka = \alpha, kb = \beta, kg = G, kh = H$ Eq. (3.12).

$$\begin{aligned} \left(\frac{R_m}{\rho c A}\right) = \frac{1}{2\pi\alpha\beta} \{4C(H,G) - 2C(H-\alpha,G) - 2C(H,G-\beta) \\ - 2C(H,G+\beta) - 2C(H+\alpha,G) \\ + C(H-\alpha,G+\beta) + C(H-\alpha,G-\beta) \\ + C(H+\alpha,G-\beta) + C(H+\alpha,G+\beta) \end{aligned} \tag{3.12}$$

where, $C(x, y)$ function is Eq. (3.13) [10].

$$
\begin{aligned}
C(x,y) = |x| \int_{|y|}^{(x^2+y^2)^{\frac{1}{2}}} & \frac{\cos r}{r}(r^2-y^2)^{\frac{1}{2}} dr \\
+ |y| \int_{|x|}^{(x^2+y^2)^{\frac{1}{2}}} & \frac{\cos r}{r}(r^2-x^2)^{\frac{1}{2}} dr \\
- \cos(x^2+y^2)^{\frac{1}{2}} & - (x^2+y^2)^{\frac{1}{2}} \sin(x^2+y^2)^{\frac{1}{2}}
\end{aligned}
\tag{3.13}
$$

The mutual radiation reactance X_m is divided by $\rho c A$ and it has the same formulation as in Eq. (3.12), however $C(x, y)$ is substituted by $S(x, y)$, which is Eq. (3.14) [10].

$$
\begin{aligned}
S(x,y) = -|x| \int_{|y|}^{(x^2+y^2)^{\frac{1}{2}}} & \frac{\sin r}{r}(r^2-y^2)^{\frac{1}{2}} dr \\
- |y| \int_{|x|}^{(x^2+y^2)^{\frac{1}{2}}} & \frac{\sin r}{r}(r^2-x^2)^{\frac{1}{2}} dr \\
- (x^2+y^2)^{\frac{1}{2}} \cos(x^2+y^2)^{\frac{1}{2}} & + \sin(x^2+y^2)^{\frac{1}{2}}
\end{aligned}
\tag{3.14}
$$

The quadruple integral of mutual radiation impedance becomes Eq. (3.12), which consists of integrals of single variable together with the integrated expressions of these steps. Then, evaluation of the mutual radiation resistance and reactance reduces to numerical integration calculations.

The above integrations are implemented and the results are plotted in Fig. 3.4 and Fig. 3.5, which are similar to the work in [10]. For small distances between the elements, impedance values are not small compared to the values of distant elements of kd. It is obvious that impedances oscillate around zero and then they converge to zero.

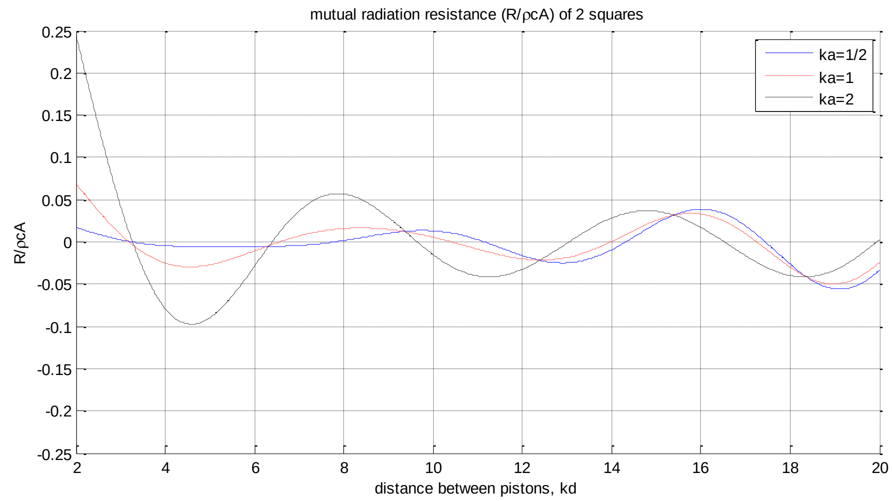

Figure 3.4: Mutual radiation resistance ($R/\rho cA$) of two square pistons with distance kd and element dimensions ka

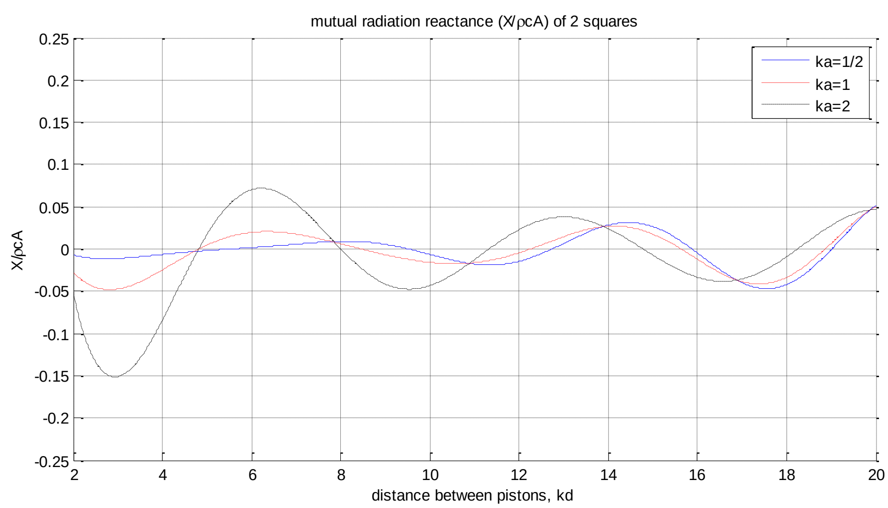

Figure 3.5: Mutual radiation reactance ($X/\rho cA$) of two square pistons with distance kd and element dimensions ka

Chapter 4

Mutual Impedance Considerations

4.1 Mutual Impedance Checksum

In planar acoustic arrays, applications and simulations are generally based on element characteristics. However, in this research, it is shown that there is also an effect of mutual interactions. In Fig. 4.1, there are four square pistons with side length a, and suppose that there is one larger square piston with side length $2a$, which is actually filled with the four of these smaller pistons. Larger piston's self-radiation impedance can be calculated by the self-radiation impedance and mutual radiation impedance of those smaller pistons.

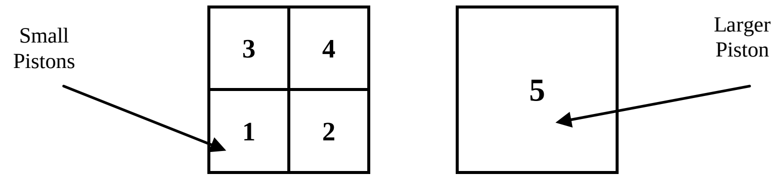

Figure 4.1: Arrangement of pistons for superposition principle

In a rigid baffle, Eq. (4.1) is the pressure and particle velocity relation of four pistons. The particle velocity is the same for all smaller pistons and the larger one U_1=U_2=...=U_5 $= U$. On the other hand, the total radiation area of the smaller pistons are equal to the radiation area of the larger piston, which gives us $F_5 = \sum_{i=1}^{4} F_i$ as force values. Thus, multiplying both sides of Eq. (4.1) with [1 1 1 1] and then, in order to get impedance values, dividing F to U results as the first part of Eq. (4.2).

$$\begin{bmatrix} F_1 \\ F_2 \\ F_3 \\ F_4 \end{bmatrix} = \begin{bmatrix} Z_{11} & Z_{12} & Z_{13} & Z_{14} \\ Z_{21} & Z_{22} & Z_{23} & Z_{24} \\ Z_{31} & Z_{32} & Z_{33} & Z_{34} \\ Z_{41} & Z_{42} & Z_{43} & Z_{44} \end{bmatrix} \begin{bmatrix} U_1 \\ U_2 \\ U_3 \\ U_4 \end{bmatrix} \tag{4.1}$$

In Fig. 4.2 and Fig. 4.3, kd=0 shows the self-radiation impedance of the small piston, kd=ka is the mutual radiation impedance of two adjacent pistons. kd=$s2ka$ line is the mutual radiation impedance of crosswise located small pistons and finally, $ka2$ is the larger piston's self-radiation impedance.

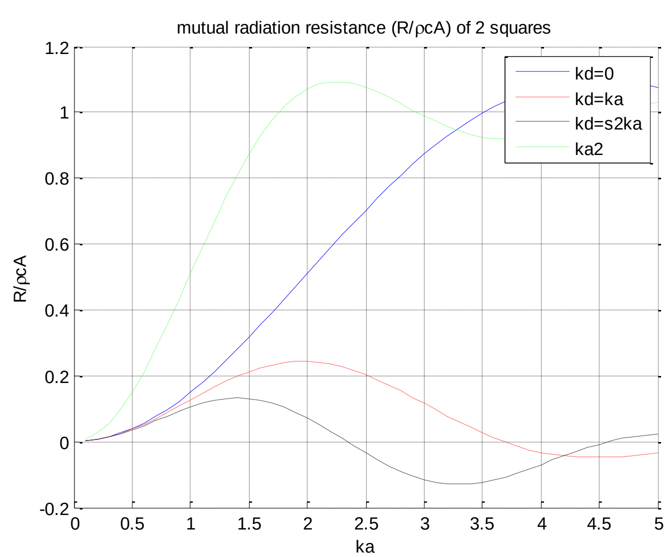

Figure 4.2: Self and mutual radiation resistance ($R/\rho cA$) relations with element dimension ka

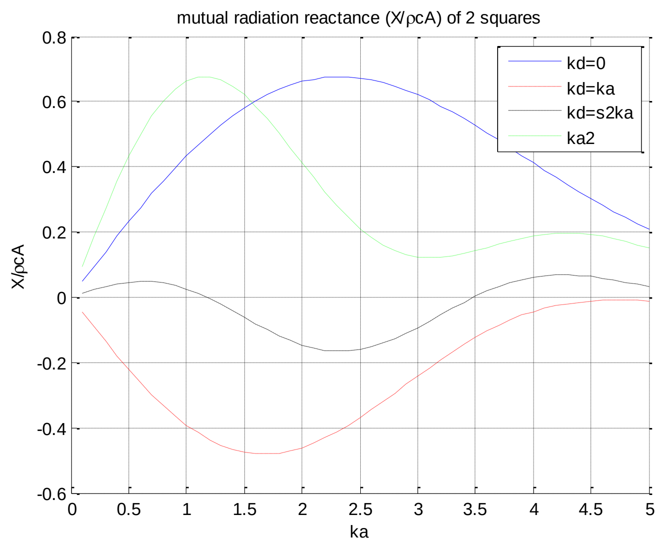

Figure 4.3: Self and mutual radiation reactance $(X/\rho cA)$ relations with element dimension ka

Indeed, these impedance relations are demonstrated as mutual radiation resistance and reactance in Fig. 4.2 and Fig. 4.3, respectively. Because of the symmetry of square geometry, these four different relations suffice to calculate the self-radiation impedance of the large piston from the smaller pistons.

$$Z_5 = \sum_{i=1}^{4} Z_{i,i} + \sum_{i,j} Z_{i,j} = 4Z_{1,1} + 84Z_{1,2} + 4Z_{1,4} \tag{4.2}$$

In practical calculations, Eq. (4.2) describes how piston calculations are done with the superposition principle. Actually, the main idea is combining all possible dual relations of small pistons plus their self-radiation impedances. Using the symmetry of array, $Z_{1,1}$ is same for all four small pistons. $Z_{1,2}$ is added 8 times, since there are 8 adjacent mutual impedance data input and $Z_{1,4}$ is counted 4 times as it is the same for all diagonally located pistons. As we add them numerically and check against the larger piston, the error rate is smaller than 10^{-5}, as shown in Fig. 4.4. For a graphical demonstration, larger square's self-radiation impedance and superposition results are plotted together. The result indicates that they fit perfectly, as expected.

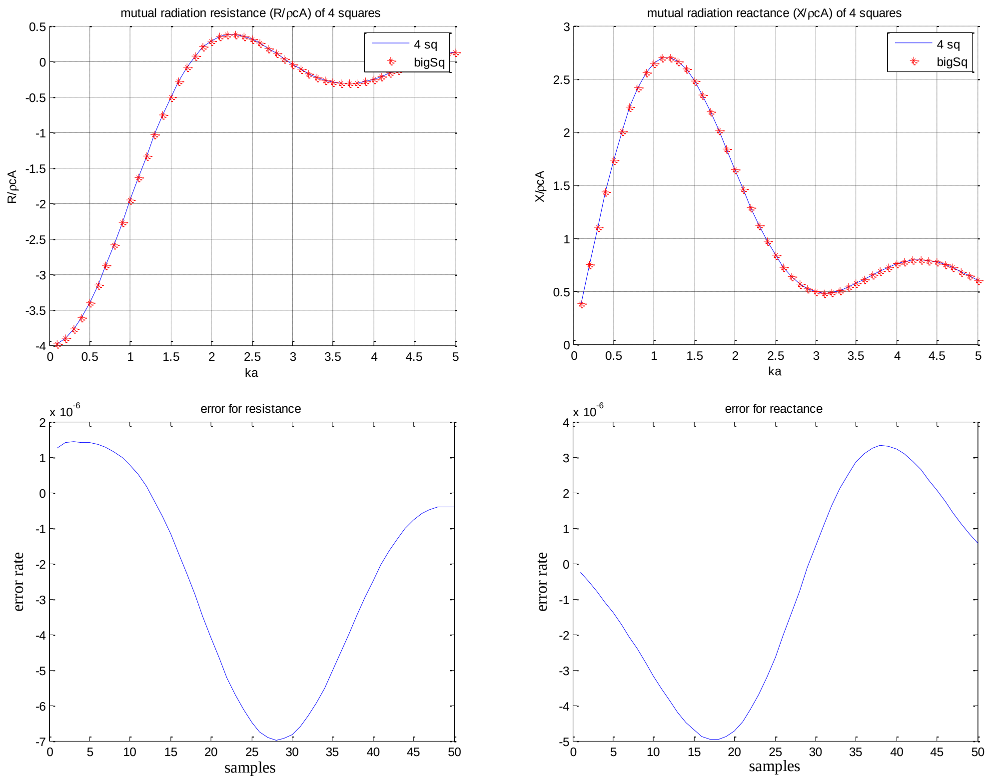

Figure 4.4: Self and mutual radiation error rates

4.2 Checksum of Squares Spread over the Baffle

Arrays generally have more than four elements. In order to see the real time operation of an array, the number of elements is increased and the calculations are made upon those elements.

A procedure is followed as in Section 4.1. A Matlab program is coded for a generic array of n^2 elements, where there are n elements on each column of the array [25]. First, we calculate each element's self-radiation impedance, which is identical for all. Then for any two different elements on the array, the mutual radiation impedance is calculated and added to the self-radiation impedances.

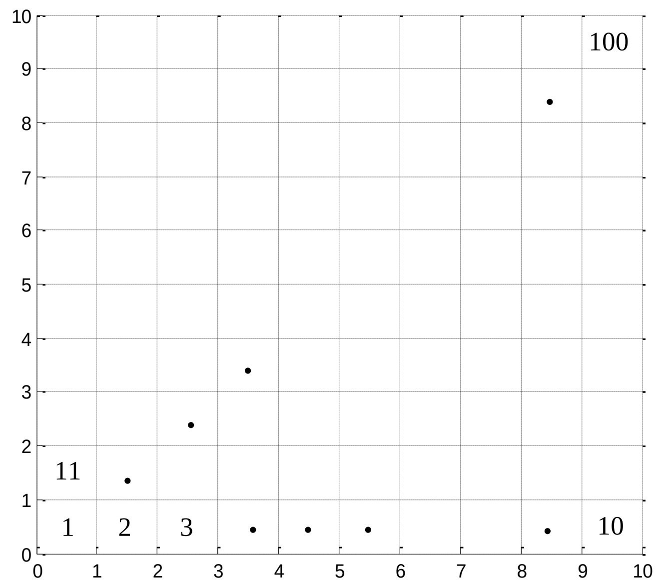

Figure 4.5: Setting of an array with n^2=100 elements

This summation is expected to be close to the self-radiation impedance of the square piston whose radiation area is equal to n^2 elements total radiation area.

This superposition method proves that our technique for self and mutual radiation impedance calculations are accurate. Indeed, the error rate for n=10 and $ka = 0.1$ is smaller than 0.001 and for $ka = [1, \pi/2, 2]$, rates are smaller than 0.0001 where the array setting in Fig. 4.5 is used for this case. This method also gives us the opportunity of having a missing mutual impedance data if needed.

4.3 Mutual Impedance Effect of an Element over the Array

Up to this section, interactions between elements are observed and accurate calculations are done. However, effect of a single element on the whole array is not given. Consider an array, that has many elements and its signal needs beam forming for a special application. If we can inspect one element's possible effect over the array, then to remove that effect adjusting the other elements is easy and the inputs of those elements can be set again to form the desired beam.

In this section, we take an array of n elements in a rigid baffle again. To achieve symmetry and to be able to use the center element, n is assumed to be odd. The elements are considered to operate simultaneously. Only the center piston is shut down. For every element, the mutual impedance effect between that element and the center element can be seen with this setup.

0,056241	0,035496	0,08639	0,024042	0,059309	0,019661	0,035822	0,009394	0,013492	0,015252	0,013492	0,009394	0,035822	0,019661	0,059309	0,024042	0,08639	0,035496	0,056241
0,035496	0,074592	0,065585	0,02994	0,057794	0,012675	0,040891	0,002288	0,006937	0,019551	0,006937	0,002288	0,040891	0,012675	0,057794	0,02994	0,065585	0,074592	0,035496
0,08639	0,065585	0,042538	0,059044	0,058776	0,018253	0,037701	0,012253	0,013021	0,015849	0,013021	0,012253	0,037701	0,018253	0,058776	0,059044	0,042538	0,065585	0,08639
0,024042	0,02994	0,059044	0,078979	0,05439	0,035014	0,035261	0,023369	0,018071	0,019413	0,018071	0,023369	0,035261	0,035014	0,05439	0,078979	0,059044	0,02994	0,024042
0,059309	0,057794	0,058776	0,05439	0,042079	0,065057	0,039109	0,030426	0,011044	0,031297	0,011044	0,030426	0,039109	0,065057	0,042079	0,05439	0,058776	0,057794	0,059309
0,019661	0,012675	0,018253	0,035014	0,065057	0,073682	0,028395	0,051244	0,010152	0,041266	0,010152	0,051244	0,028395	0,073682	0,065057	0,035014	0,018253	0,012675	0,019661
0,035822	0,040891	0,037701	0,035261	0,039109	0,028395	0,054193	0,079127	0,004772	0,059508	0,004772	0,079127	0,054193	0,028395	0,039109	0,035261	0,037701	0,040891	0,035822
0,009394	0,002288	0,012253	0,023369	0,030426	0,051244	0,079127	0,060992	0,045906	0,09278	0,045906	0,060992	0,079127	0,051244	0,030426	0,023369	0,012253	0,002288	0,009394
0,013492	0,006937	0,013021	0,018071	0,011044	0,010152	0,004772	0,045906	0,176017	0,151973	0,176017	0,045906	0,004772	0,010152	0,011044	0,018071	0,013021	0,006937	0,013492
0,015252	0,019551	0,015849	0,019413	0,031297	0,041266	0,059508	0,09278	0,151973	0	0,151973	0,09278	0,059508	0,041266	0,031297	0,019413	0,015849	0,019551	0,015252
0,013492	0,006937	0,013021	0,018071	0,011044	0,010152	0,004772	0,045906	0,176017	0,151973	0,176017	0,045906	0,004772	0,010152	0,011044	0,018071	0,013021	0,006937	0,013492
0,009394	0,002288	0,012253	0,023369	0,030426	0,051244	0,079127	0,060992	0,045906	0,09278	0,045906	0,060992	0,079127	0,051244	0,030426	0,023369	0,012253	0,002288	0,009394
0,035822	0,040891	0,037701	0,035261	0,039109	0,028395	0,054193	0,079127	0,004772	0,059508	0,004772	0,079127	0,054193	0,028395	0,039109	0,035261	0,037701	0,040891	0,035822
0,019661	0,012675	0,018253	0,035014	0,065057	0,073682	0,028395	0,051244	0,010152	0,041266	0,010152	0,051244	0,028395	0,073682	0,065057	0,035014	0,018253	0,012675	0,019661
0,059309	0,057794	0,058776	0,05439	0,042079	0,065057	0,039109	0,030426	0,011044	0,031297	0,011044	0,030426	0,039109	0,065057	0,042079	0,05439	0,058776	0,057794	0,059309
0,024042	0,02994	0,059044	0,078979	0,05439	0,035014	0,035261	0,023369	0,018071	0,019413	0,018071	0,023369	0,035261	0,035014	0,05439	0,078979	0,059044	0,02994	0,024042
0,08639	0,065585	0,042538	0,059044	0,058776	0,018253	0,037701	0,012253	0,013021	0,015849	0,013021	0,012253	0,037701	0,018253	0,058776	0,059044	0,042538	0,065585	0,08639
0,035496	0,074592	0,065585	0,02994	0,057794	0,012675	0,040891	0,002288	0,006937	0,019551	0,006937	0,002288	0,040891	0,012675	0,057794	0,02994	0,065585	0,074592	0,035496
0,056241	0,035496	0,08639	0,024042	0,059309	0,019661	0,035822	0,009394	0,013492	0,015252	0,013492	0,009394	0,035822	0,019661	0,059309	0,024042	0,08639	0,035496	0,056241

Figure 4.6: Mutual radiation effect of the center element

In Fig. 4.6, the array have n^2=361 elements (n=19). Color concentrated values in each cell describe the absolute value of current mutual radiation impedance between that cell and the center cell, which is normalized to 1. Values are faded away as the distance between the element and the center element increases. For a fair amount of distance mutual radiation effects shall be omitted, which is for $ka > 5$. It is also obvious on the figure that, the effect fades away more slowly on the diagonal entries. Consider the cross section of the center element, where diagonally its length is $a\sqrt{2}$ and horizontally/vertically a. Diagonal cross section is longer, which shall cause the diagonal elements are affected more.

4.4 Mutual Impedance Effect of Four Elements over the Array

Following the approach in the previous section, the effect of four elements is shown in this section. In this case, there are four elements at the center of the array. Using this application, the effect over four elements is presented. This is indeed a way of considering the effect over the area of elements, not just one element of the array.

0,2359	0,1771	0,1395	0,2252	0,1141	0,339	0,4478	0,6034	0,6034	0,4478	0,339	0,1141	0,2252	0,1395	0,1771	0,2359
0,1771	0,316	0,3325	0,1263	0,1664	0,203	0,5224	0,5871	0,5871	0,5224	0,203	0,1664	0,1263	0,3325	0,316	0,1771
0,1395	0,3325	0,14	0,3405	0,0853	0,1619	0,3446	0,3464	0,3464	0,3446	0,1619	0,0853	0,3405	0,14	0,3325	0,1395
0,2252	0,1263	0,3405	0,2783	0,3617	0,3016	0,2204	0,5853	0,5853	0,2204	0,3016	0,3617	0,2783	0,3405	0,1263	0,2252
0,1141	0,1664	0,0853	0,3617	0,0877	0,4554	0,4854	0,5786	0,5786	0,4854	0,4554	0,0877	0,3617	0,0853	0,1664	0,1141
0,339	0,203	0,1619	0,3016	0,4554	0,1543	0,4224	0,299	0,299	0,4224	0,1543	0,4554	0,3016	0,1619	0,203	0,339
0,4478	0,5224	0,3446	0,2204	0,4854	0,4224	0,6882	0,1146	0,1146	0,6882	0,4224	0,4854	0,2204	0,3446	0,5224	0,4478
0,6034	0,5871	0,3464	0,5853	0,5786	0,299	0,1146	0	0	0,1146	0,299	0,5786	0,5853	0,3464	0,5871	0,6034
0,6034	0,5871	0,3464	0,5853	0,5786	0,299	0,1146	0	0	0,1146	0,299	0,5786	0,5853	0,3464	0,5871	0,6034
0,4478	0,5224	0,3446	0,2204	0,4854	0,4224	0,6882	0,1146	0,1146	0,6882	0,4224	0,4854	0,2204	0,3446	0,5224	0,4478
0,339	0,203	0,1619	0,3016	0,4554	0,1543	0,4224	0,299	0,299	0,4224	0,1543	0,4554	0,3016	0,1619	0,203	0,339
0,1141	0,1664	0,0853	0,3617	0,0877	0,4554	0,4854	0,5786	0,5786	0,4854	0,4554	0,0877	0,3617	0,0853	0,1664	0,1141
0,2252	0,1263	0,3405	0,2783	0,3617	0,3016	0,2204	0,5853	0,5853	0,2204	0,3016	0,3617	0,2783	0,3405	0,1263	0,2252
0,1395	0,3325	0,14	0,3405	0,0853	0,1619	0,3446	0,3464	0,3464	0,3446	0,1619	0,0853	0,3405	0,14	0,3325	0,1395
0,1771	0,316	0,3325	0,1263	0,1664	0,203	0,5224	0,5871	0,5871	0,5224	0,203	0,1664	0,1263	0,3325	0,316	0,1771
0,2359	0,1771	0,1395	0,2252	0,1141	0,339	0,4478	0,6034	0,6034	0,4478	0,339	0,1141	0,2252	0,1395	0,1771	0,2359

Figure 4.7: Mutual radiation effect of four elements at the center

In Fig. 4.7, the array has n^2=256 elements (n=16). Color concentrated values in each cell describe the absolute value of current mutual radiation impedance between that cell and the center cells, which is normalized to 1. Values fade away as the distance between the element and the center elements increases. For a fair amount of distance, mutual radiation effects shall be omitted, which is for $ka > 5$. It is also obvious from Fig. 4.7 that, the effect fades away more slowly on horizontal and vertical entries this time. The reason for this phenomenon can be explained by the usage of four center elements as a reference point.The radiation area of four-element center pistons is four times bigger than any other elements. This difference between the areas causes deep effects on other transducers, then the coupling effect shall be stronger on the main directions.

Chapter 5

Generic Model Simulation

5.1 A Generic Model for Array Elements

In this chapter, we present a generic equivalent circuit model for the square piston element of a planar acoustic array in order to observe the effects of underwater medium loading. The transducer is assumed lossless and hence the resistive elements are omitted in the model. The interactions between the elements of planar acoustic array are analyzed using this generic equivalent circuit model. While operating the array, each element generates a pressure field that act upon the others. This effect is represented by the mutual radiation impedance between the elements. The planar acoustic array of square piston elements is analyzed by simulating the model in Matlab [25]. Linear frequency domain response of the array can be obtained very rapidly simulating this model.

The generic equivalent circuit model for the square piston element of a planar acoustic array is shown in Fig. 5.1. This basic linear circuit can model the motion of the piston transducer. It contains the electrical port as a voltage source and at the mechanical port radiation impedance of the transducer is modeled, which can be calculated from the transducer's characteristics.

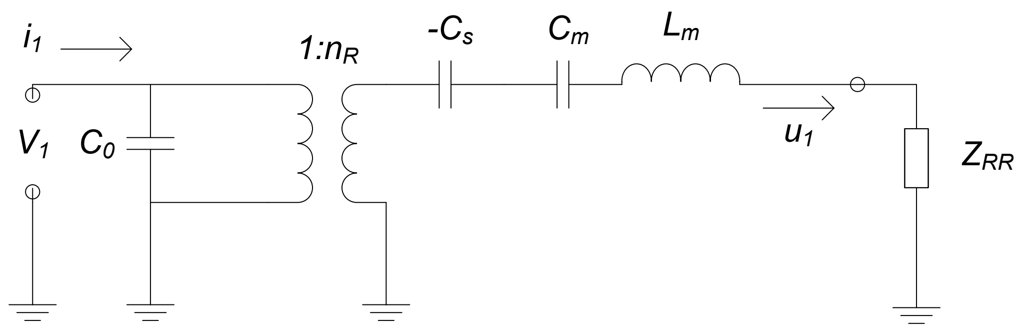

Figure 5.1: Generic equivalent circuit model of the square piston element

This small signal equivalent circuit model contains generic elements for a single transducer. C_m stands for the compliance of the ceramic block. L_m comes from the weight of the transducer. C_0 is also needed unless open voltage and short circuit reception cases may be differentiate. The model includes a transformer with turns ratio n_R. C_s is the counterpart of C_0 at mechanical side. V_1 and i_1 are voltage and circuit at electrical side. u_1 is the particle velocity of this single transducer where Z_{RR} is the radiation impedance. All these elements are defined in the parameters of quality factor Q and resonance frequency w_r while the other constants are fixed by the environment. All the defined parameters can be found in the Appendix A.

Consider an n-by-n array that contains n^2=N square piston elements in a rigid baffle. The array is immersed in a liquid medium. As it is shown in Fig. 5.2, mechanical ports of all N elements are connected to the Z matrix, which has N ports for self and mutual radiation impedance values for each element. The diagonal entries of the Z matrix contains the self-radiation impedances of the elements and the remaining parts of the matrix are mutual radiation impedances as stated in the previous chapters. There are voltage sources for each element that connected directly to the models and $V_{in1}, V_{in2}, ..., V_{inN}$ are the phasors of the sources.

In order to find the element velocities, each equation needs to be solved. The input current value for each element is found. Then, conductance and susceptance

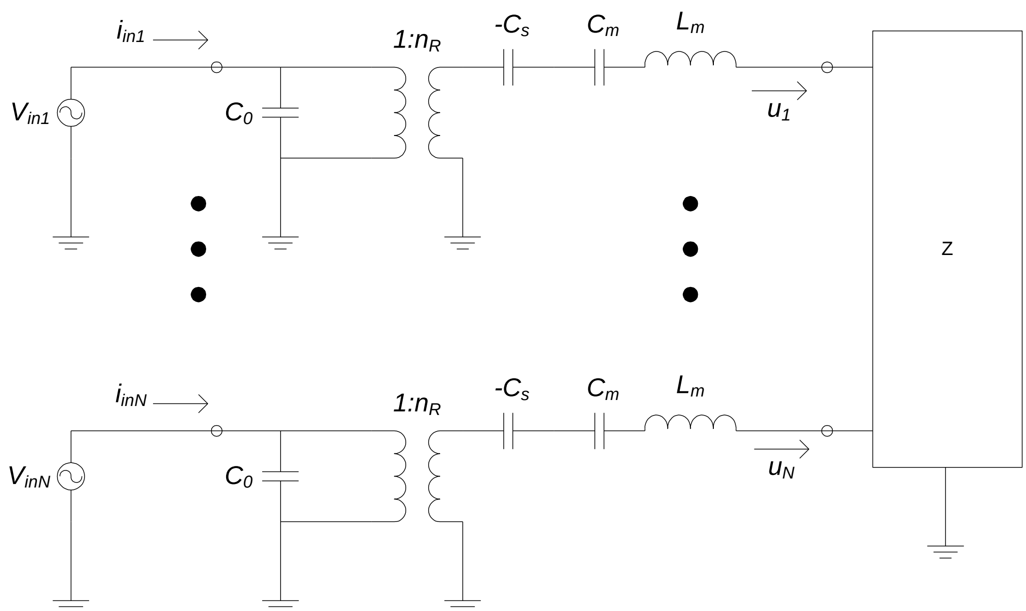

Figure 5.2: Generic equivalent circuit model of the square piston elements of a planar acoustic array

with respect to frequency for different elements can be calculated and plotted.

$$\begin{aligned} n_R V_p = \big[jwL_m + \frac{1}{jw}\big(\frac{1}{C_m} - \frac{1}{C_s}\big) + Z_{RR}(ka) \big] u_p \\ + \sum_{q=1, q\neq p}^{N} Z_M(ka, kd_{pq}) u_p, \;\; p{=}1, 2, ..., N \end{aligned} \tag{5.1}$$

There are N equations for every element. Since, they are in order, they can be written in a matrix form. $n_R V = M(w)u$ is the simple formation where V is the column vector for voltages, V_p, and u is for the velocities u_p as $p{=}1, 2, ..., N$. $M(w)$ is the matrix for the elements which also contains the self and mutual radiation impedances. The basis of the calculations depends on these equations. The details of the calculation steps and the Matlab code can be found in Appendix B.

A Matlab code is generated for these calculations and all the array operations are done efficiently. The code also have the flexibility that all the power, current, conductance and other related data can be calculated easily. The simulations are performed on a 10-by-10 planar square array of piston elements, as shown in Fig. 5.3. Elements that are placed in different parts of the array do not have the same frequency response, which is also seen from the inspected elements.

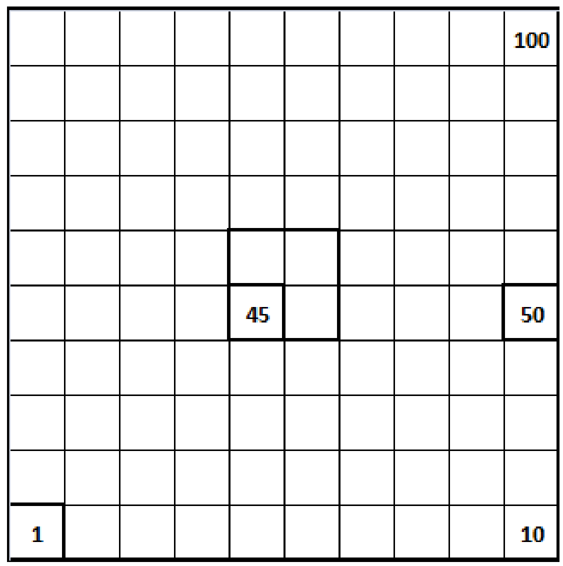

Figure 5.3: 10-by-10 planar acoustic array of piston elements

5.2 Simulation Results of the Array

In this particular work, simulations are run for the entire array; however, three elements are presented which are located at three specific positions of the array. One of the elements is located at the corner of the array (#1). Another element is chosen from center of the array (#45). Finally, the last element is picked from the edge of the array, which is actually in the middle of the chosen edge (#50). Actually, there are four different element locations for the specified positions (eight for the edge), however all of them are symmetric; then choosing one of them does not affect the calculations.

Another parameter for the simulations is the quality factor (Q) of the mechanical resonance for the driven generic models. The results for Q=5, Q=3, Q=2 and

Q=1 can be observed from the graphics of each element. In Fig. 5.4, "Conductance vs. Frequency" plots and in Fig. 5.5, "Susceptance vs. Frequency" plots of the corner element (#1) for different Q values are plotted respectively. Mechanical resonance of the system can change for different Q values. For example, at higher values of Q, the peak of response is very narrow. It climbs up to a high conductance in a small frequency window and then climbs down rapidly again. For low quality factor, there is low mechanical impedance that mutual acoustic interactions can be affected crucially. This can result as a decrease in acoustic power radiation and change the beam pattern in an undesired way. Furthermore, electromechanical transducers might not work properly.

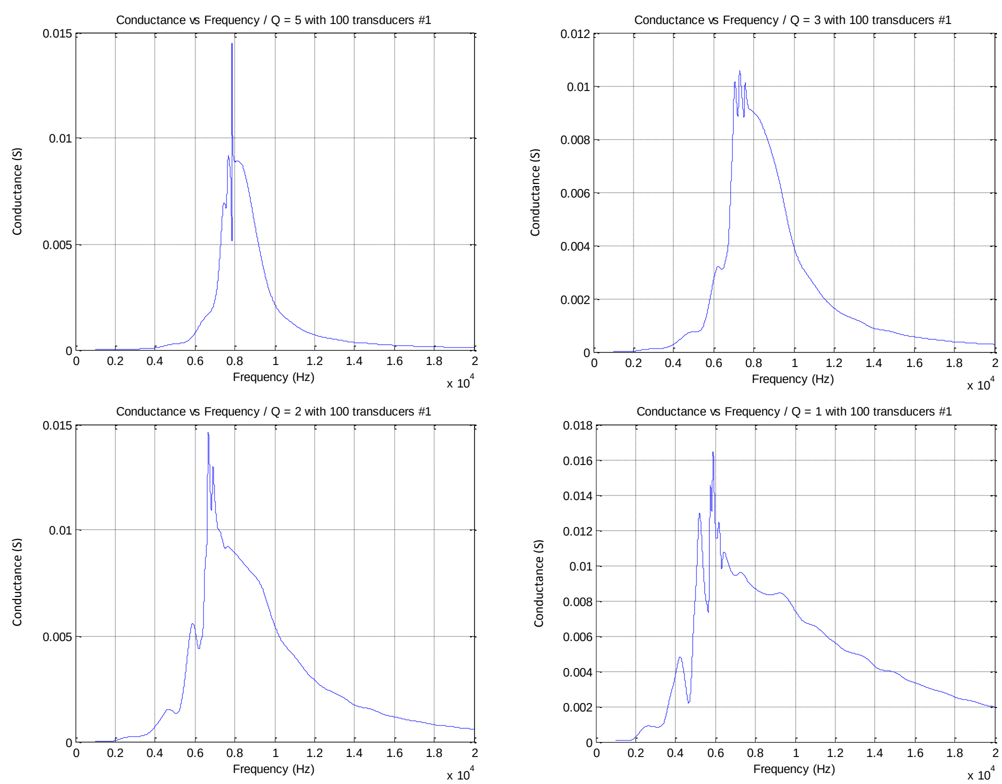

Figure 5.4: Conductance vs Frequency of the corner (#1) element

In larger arrays, quality factor (Q) is not the only factor that affects the mechanical resonance. Transducer elements that are located in different parts of the array can have different frequency responses. If the distance between the elements is larger than $\lambda/2$, then the effect of mutual acoustic interactions

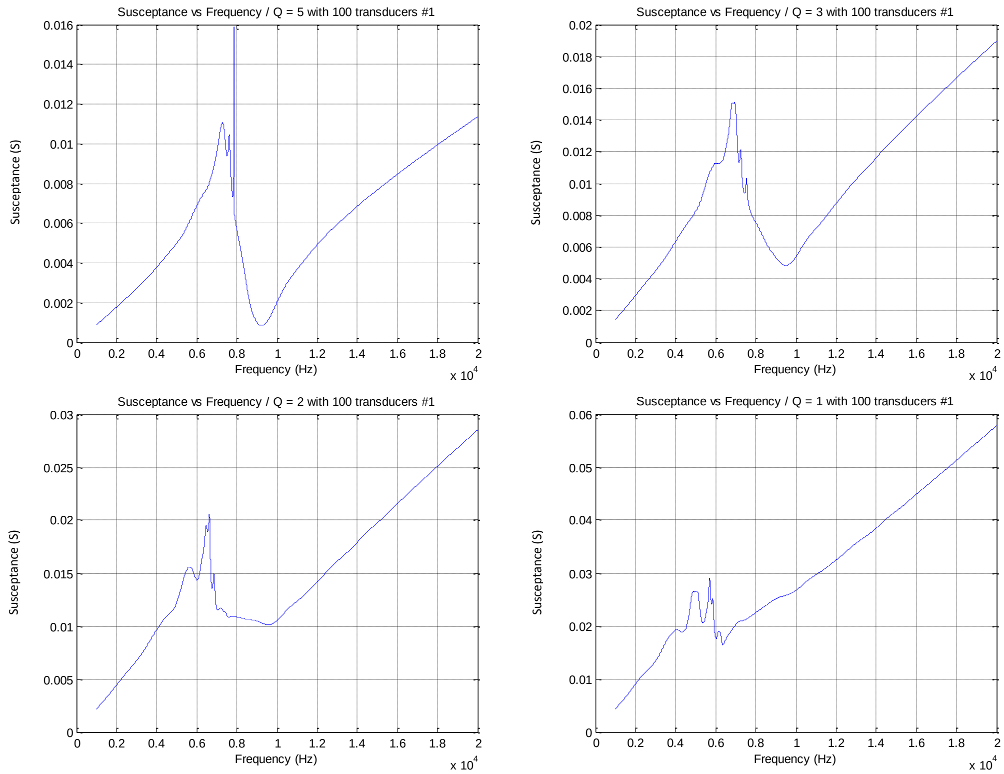

Figure 5.5: Susceptance vs Frequency of the corner (#1) element

helps the corresponding elements operation. When elements next to each other examined, these elements work in a more constrained situation. It is also same for other element couples, which have a distance of $3\lambda/2$ between them. This effect can be described as if some other force pulls or pushes the corresponding element due to other elements, which in turn causes mutual acoustic interactions. Considering the whole array and combined effects of all elements on each other, this becomes a pushing and pulling through the medium effect. Resulting effect causes a mechanical resonance. Generally, the mechanical resonance occurs just beneath the resonance frequency. Meanwhile, the whole array has this effect and each element is affected individually, depending on its position in the array. Then, the output beam generated from the array has very diverse results.

The mechanical resonance effect travels through elements as a wave motion. When this wave effect reaches to the rigid edge of the array, it reflects back and then this situation results in a new resonance effect. Other than the first pushing and pulling through the medium effect, now there is a mechanical resonance on the horizontal/vertical axes. Having both effects at the same time is actually Rayleigh-Bloch effect, which is also observed in CMUTs [26]. In Fig. 5.6, frequency responses of the corner (#1), the center (#45) and the edge (#50) elements are depicted respectively with a quality factor (Q) of 2. It can easily be seen that distortion occurs below the resonance frequency 8.5 MHz. The effect of the mutual acoustic interactions is also more evident for the corner and the edge elements, where the center element has also this effect but it passes the relevant frequencies more smoothly. In Fig. 5.7, frequency responses of these three elements are plotted with Q=5. The distortion still exists and the acoustic coupling is still effective. However, for Q=5, we have more reliable results since those effects are weaker than the case when Q=2. Plots for other quality factors can be found in Appendix C.

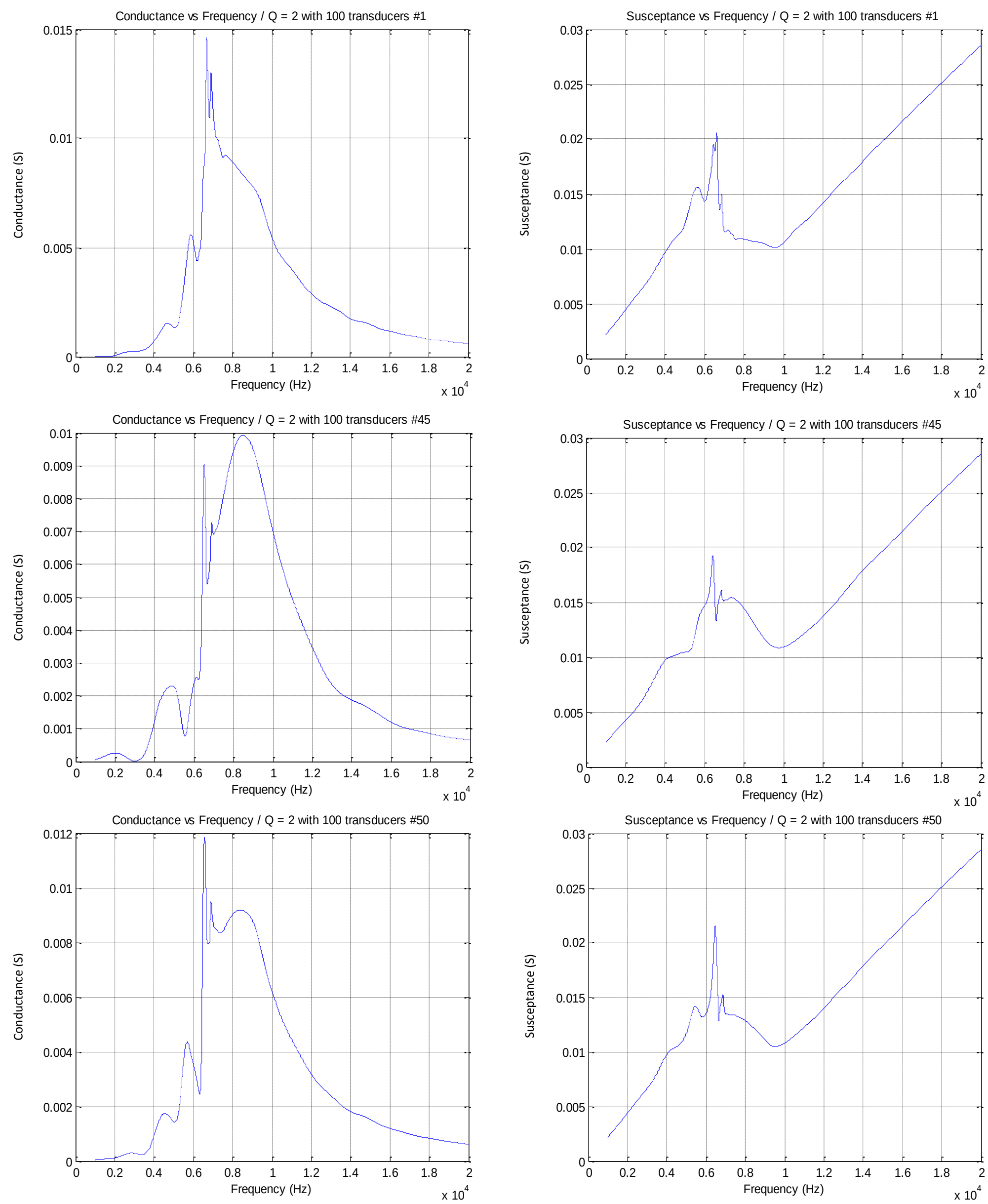

Figure 5.6: Conductance/Susceptance vs Frequency of the corner (#1), center (#45) and edge (#50) elements with quality factor Q=2

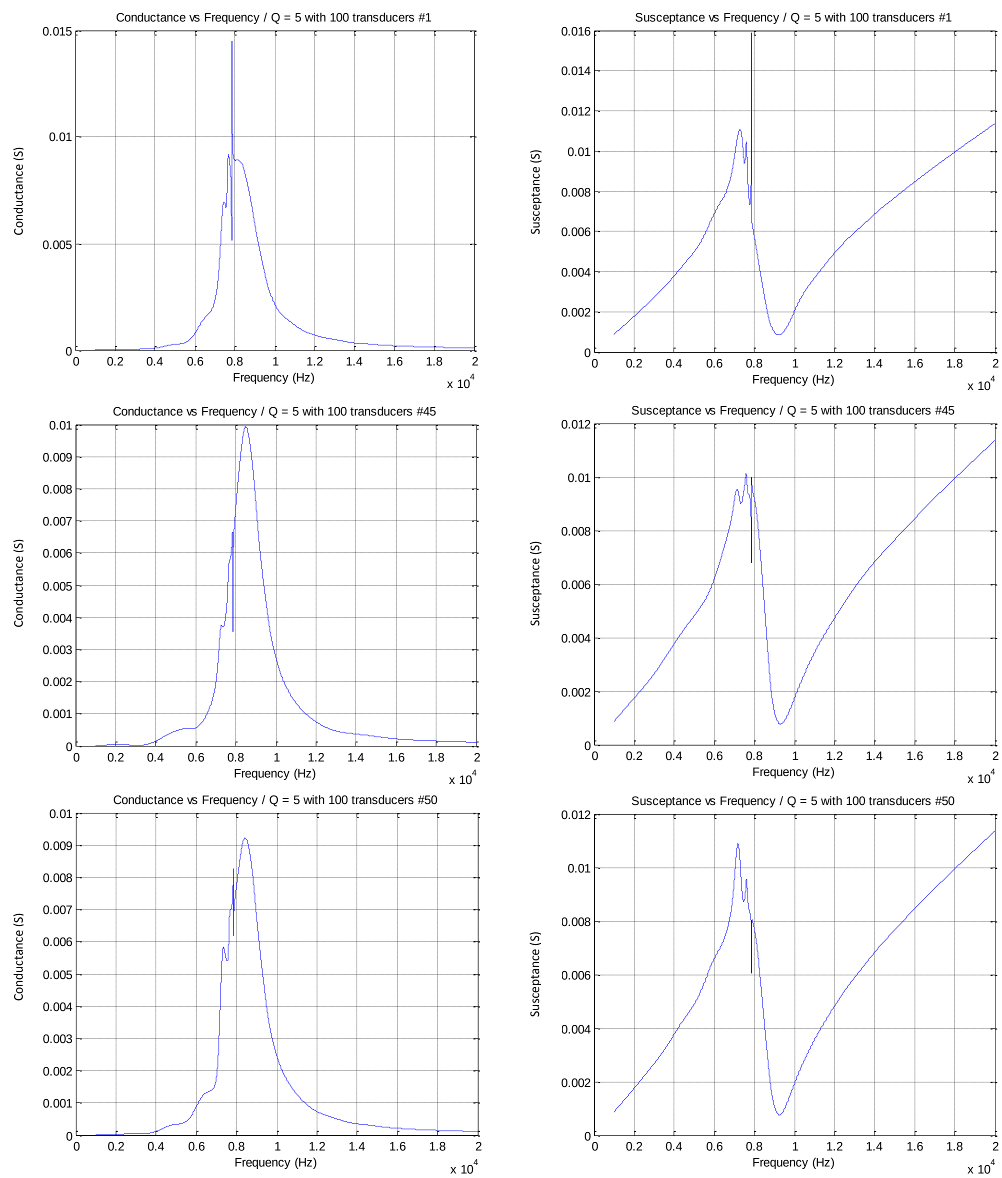

Figure 5.7: Conductance/Susceptance vs Frequency of the corner (#1), center (#45) and edge (#50) elements with quality factor Q=5

Chapter 6

Conclusion

Large acoustic arrays are an indispensible part of many military and civil underwater applications. In this thesis, a method for predicting the effects of mutual acoustic coupling by using the mutual radiation impedances of transducers is presented. We focused on square piston elements on two-dimensional planar acoustic arrays. We presented the array concept and its implementation for acoustic systems. We also gave basic information on the acoustic environments.

We presented the projection of possible acoustic couplings on two-dimensional planar acoustic arrays by using the mutual radiation impedance information, which is gathered from the design parameters of the array. A mutual impedance checksum is also done with the elements of an array. Next, the acoustic coupling effect of a single element on the other elements of the array is calculated and presented with a color concentrated figure. Moreover, an array, whose center has four elements, is studied and the same steps are repeated for this case.

We implemented a generic equivalent circuit model for the piston transducer. The frequency response of an array, which is built with these elements, is simulated by driving this circuit model. Conductance and susceptance values are plotted with respect to frequency. The change of resonance is inspected by the quality factor (Q). The results vary for elements located in different locations of the array. The effects of mutual impedance interactions are observed for every case simulated. It is also found that the output of the signal is a Raleigh-Bloch wave, similar as in CMUTs.

As future work, real-time beam forming changes can be studied under the vision of this work and solutions for well-formed beams can be configured. The effect of interelement coupling through the medium can be studied on imaging performance of acoustic imaging devices by extending the concept and the techniques presented here.

Bibliography

[1] D. L. Carson, "Diagnosis and cure of erratic velocity distributions in sonar projector arrays," *The Journal of the Acoustical Society of America*, vol. 34, no. 9A, pp. 1191–1196, 1962.

[2] H. K. Oğuz, S. Olcum, M. N. Şenlik, V. Taş, A. Atalar, and H. Köymen, "Nonlinear modeling of an immersed transmitting capacitive micromachined ultrasonic transducer for harmonic balance analysis," *Ultrasonics, Ferroelectrics, and Frequency Control, IEEE Transactions on*, vol. 57, no. 2, pp. 438–447, 2010.

[3] S. Olcum, F. Y. Yamaner, A. Bozkurt, H. Köymen, and A. Atalar, "An equivalent circuit model for transmitting capacitive micromachined ultrasonic transducers in collapse mode," *Ultrasonics, Ferroelectrics, and Frequency Control, IEEE Transactions on*, vol. 58, no. 7, pp. 1468–1477, 2011.

[4] A. Caronti, D. Fiasca, G. Caliano, M. Pappalardo, and E. Cianci, "Experimental study of acoustic coupling in CMUT arrays by optical interferometry," in *Ultrasonics, 2003 IEEE Symposium on*, vol. 2, pp. 1960–1969, IEEE, 2003.

[5] A. Caronti, A. Savoia, G. Caliano, and M. Pappalardo, "Acoustic coupling in capacitive microfabricated ultrasonic transducers: Modeling and experiments," *Ultrasonics, Ferroelectrics, and Frequency Control, IEEE Transactions on*, vol. 52, no. 12, pp. 2220–2234, 2005.

[6] S. Zhou, J. Hossack, *et al.*, "Reducing inter-element acoustic crosstalk in capacitive micromachined ultrasound transducers," *Ultrasonics, Ferroelectrics,*

and Frequency Control, IEEE Transactions on, vol. 54, no. 6, pp. 1217–1228, 2007.

[7] H. K. Oğuz, A. Atalar, and H. Köymen, "Equivalent circuit-based analysis of CMUT cell dynamics in arrays," *Ultrasonics, Ferroelectrics, and Frequency Control, IEEE Transactions on*, vol. 60, no. 5, pp. 1016–1024, 2013.

[8] K. Sha, J. Yang, and W.-S. Gan, "A simple calculation method for the self- and mutual-radiation impedance of flexible rectangular patches in a rigid infinite baffle," *Journal of sound and vibration*, vol. 282, no. 1, pp. 179–195, 2005.

[9] G. W. Swenson Jr and W. E. Johnson, "Radiation impedance of a rigid square piston in an infinite baffle," *The Journal of the Acoustical Society of America*, vol. 24, no. 1, pp. 84–84, 1952.

[10] E. M. Arase, "Mutual radiation impedance of square and rectangular pistons in a rigid infinite baffle," *The Journal of the Acoustical Society of America*, vol. 36, no. 8, pp. 1521–1525, 1964.

[11] S. J. Klapman, "Interaction impedance of a system of circular pistons," *The Journal of the Acoustical Society of America*, vol. 11, no. 3, pp. 289–295, 1940.

[12] R. Pritchard, "Mutual acoustic impedance between radiators in an infinite rigid plane," *The Journal of the Acoustical Society of America*, vol. 32, no. 6, pp. 730–737, 1960.

[13] D. T. Porter, "Self-and mutual-radiation impedance and beam patterns for flexural disks in a rigid plane," *The Journal of the Acoustical Society of America*, vol. 36, no. 6, pp. 1154–1161, 1964.

[14] D. T. Porter, "Near field sound pressure on square and rectangular pistons," tech. rep., DTIC Document, 1962.

[15] R. J. Urick, "Principles of underwater sound," *New York: McGraw-Hill Book Company*, 1983.

[16] C. H. Sherman and J. L. Butler, *Transducers and arrays for underwater sound*. Springer, 2007.

[17] C. Audoly, "Some aspects of acoustic interactions in sonar transducer arrays," *The Journal of the Acoustical Society of America*, vol. 89, no. 3, pp. 1428–1433, 1991.

[18] J. Lee, I. Seo, and S.-M. Han, "Radiation power estimation for sonar transducer arrays considering acoustic interaction," *Sensors and Actuators A: Physical*, vol. 90, no. 1, pp. 1–6, 2001.

[19] H. Lee, J. Tak, W. Moon, and G. Lim, "Effects of mutual impedance on the radiation characteristics of transducer arrays," *The Journal of the Acoustical Society of America*, vol. 115, no. 2, pp. 666–679, 2004.

[20] C. H. Sherman, "Analysis of acoustic interactions in transducer arrays," *Sonics and Ultrasonics, IEEE Transactions on*, vol. 13, no. 1, pp. 9–15, 1966.

[21] D. T. Blackstock, *Fundamentals of physical acoustics*. John Wiley & Sons, 2000.

[22] C. H. Sherman, "Mutual radiation impedance of sources on a sphere," *The Journal of the Acoustical Society of America*, vol. 31, no. 7, pp. 947–952, 1959.

[23] J. E. Greenspon and C. H. Sherman, "Mutual-radiation impedance and nearfield pressure for pistons on a cylinder," *The Journal of the Acoustical Society of America*, vol. 36, no. 1, pp. 149–153, 1964.

[24] H. Köymen, "Beamforming." unpublished note, 2013.

[25] The Mathworks, Inc., Natick, Massachusetts, *MATLAB version 8.3.0.532 (R2014a)*, 2014.

[26] A. Atalar, H. Köymen, and H. K. Oğuz, "Rayleigh-Bloch waves in CMUT arrays," *Ultrasonics, Ferroelectrics, and Frequency Control, IEEE Transactions on*, vol. 61, no. 12, pp. 2139–2148, 2014.

Appendix A

Parameters of the Circuit Model

$$w_m = \sqrt{1/(L_m \times C_m)} \tag{A.1}$$

$$w_m = 2\pi \times 10^4 \text{Hz} \tag{A.2}$$

$$w_r = 0.85 \times w_m \tag{A.3}$$

$$R_r = \rho c A \tag{A.4}$$

$$Q = w_r \times L_m / R_r \tag{A.5}$$

$$L_m = Q \times \rho c A / w_r \tag{A.6}$$

$$C_m = 0.85^2 / (Q \times \rho c A \times w_r) \tag{A.7}$$

$$C_s = 3.6 \times C_m \tag{A.8}$$

Appendix B

Matlab Code for Tests

```
%calculateOutput.m
    velocities =  [];
    Pout = [];
    Iin = [];
    freq = [];

    freqmin = 1e3;
    freqmax = 20e3;
    freqinc = 0.001e3;
    nr = 10;
    numoftransducers = 100;        % should be square
    voltages = 1*ones(numoftransducers,1);
    Q = 5;
    Wm = 2*pi*10e3;
    rhocA = 1025*1500*(1500*pi/(0.85*Wm*1.1))^2;
    Lm = Q*rhocA/(0.85*Wm) *ones(numoftransducers,1);
    Cm = 0.85/(Q*rhocA*Wm) *ones(numoftransducers,1);
    Cs = 3.6*Cm;
    C0 = Cs(1,1)*nr^2;

[Pout,Iin,velocities,freq] = calculatePower(voltages,...
  freqmin,freqmax,freqinc,nr,numoftransducers,Lm,Cm,Cs,C0,Wm,rhocA);
```

```
%calculatePower.m
function [Pout,Iin,velocities,freq]=calculatePower(voltages,...
    freqmin,freqmax,freqinc,nr,numoftransducers,Lm,Cm,Cs,C0,Wm,rhocA)
    freq=freqmin : freqinc : freqmax;
    velocities =  [];
    Pout = [];
    Iin = [];
    for (w = 2*pi*freq)
        %% Calculation of M Matrix
        M=zeros(numoftransducers,numoftransducers);
        Z = calcImpedance(numoftransducers,w,Wm);
        for ii = 1:numoftransducers
            M(ii,ii) = j * w * Lm(ii,1) + (1/ (j * w * Cm(ii)))...
                - (1/ (j * w * Cs(ii))) ;
        end
        M = M + Z*rhocA;
        %% Calculation of Velocities
        vel = nr * inv(M) * voltages;
        velocities = [velocities, vel];
        %% Calculation of Currents
        curr =j*w*C0*voltages + nr * vel;
        Iin = [Iin, curr];
        %% Calculation of Power
        power = 0.5 * sum (real(voltages.*curr));
        Pout = [Pout, power];
    end
end
```

```
%calcImpedance.m
function [Z] = calcImpedance(numoftransducers,w,Wm)
    n2 = numoftransducers;
    n = sqrt(numoftransducers);
    Z = zeros(n2,n2);
    ka = w .* pi/(0.85*Wm*1.1);

kan = ka.*n;
lka = length(ka);
ress = zeros(lka,n,n,n,n);
reas = zeros(lka,n,n,n,n);
```

```
rest = zeros(n,n); reat = rest; % temporary res/rea
resska = zeros(1,lka); reaska = resska;
ressn  = zeros(1,lka); reasn  = ressn;
cnt = 0;

for kal = 1:lka
resst = 0;  reast = 0;

for i1 = 1:n
    for j1 = 1:n
        if i1 == 1 && j1 == 1
            for i2 = 1:n
                for j2 = 1:n
                    if i2 == 1 && j2 == 1
                        self1ka = radimpka(ka(kal));
                        rest(i2,j2) = real(self1ka); % res;
                        reat(i2,j2) = imag(self1ka); % rea;
                         cnt = cnt+1;
                        resst = resst + rest(i2,j2);
                        reast = reast + reat(i2,j2);
                    else
                        a = ka(kal); b = a;
                        g = a*abs(j2-j1);
                        h = a*abs(i2-i1);
                        res = 1/(2*pi*a*b)*( 4*ccc(h,g) - 2*ccc(h-a,g)...
                            - 2*ccc(h,g-b) - 2*ccc(h+a,g) - 2*ccc(h,g+b)...
                            + ccc(h-a,g-b) + ccc(h-a,g+b) + ccc(h+a,g-b)...
                            + ccc(h+a,g+b) );
                        rea = 1/(2*pi*a*b)*( 4*sss(h,g) - 2*sss(h-a,g)...
                            - 2*sss(h,g-b) - 2*sss(h+a,g) - 2*sss(h,g+b)...
                            + sss(h-a,g-b) + sss(h-a,g+b) + sss(h+a,g-b)...
                            + sss(h+a,g+b) );

                        rest(i2,j2) = res;
                        reat(i2,j2) = rea;
                        cnt = cnt + 1;
                        resst = resst + res;
                        reast = reast + rea;
                    end
                end
```

```
            end
            ress(kal,i1,j1,:,:) = rest;
            reas(kal,i1,j1,:,:) = reat;
        else
            for i2 = 1:n
                for j2 = 1:n
                    i21 = abs(i2-i1);
                    j21 = abs(j2-j1);
                    g1 = j21 + 1;
                    h1 = i21 + 1;
                    ress(kal,i1,j1,i2,j2) = rest(g1,h1);
                    reas(kal,i1,j1,i2,j2) = reat(g1,h1);

                    cnt = cnt + 1;
                    resst = resst + rest(g1,h1);
                    reast = reast + reat(g1,h1);
                end
            end
        end
    end
end
resska(kal) = resst;
reaska(kal) = reast;

selfnka = radimpka(kan(kal));
ressn(kal) = real(selfnka)*n^2; % res;
reasn(kal) = imag(selfnka)*n^2; % rea;
end          % endOf kal=1:lka for loop
for i1 = 1:n
    for j1 = 1:n
        nx = (i1-1)*n + j1;
        for i2 = 1:n
            for j2 = 1:n
                ny = (i2-1)*n + j2;
                Z(nx,ny) = ress(kal,i1,j1,i2,j2) + j* reas(kal,i1,j1,i2,j2);
            end
        end
    end
end
end
```

Appendix C

Extra Graphics

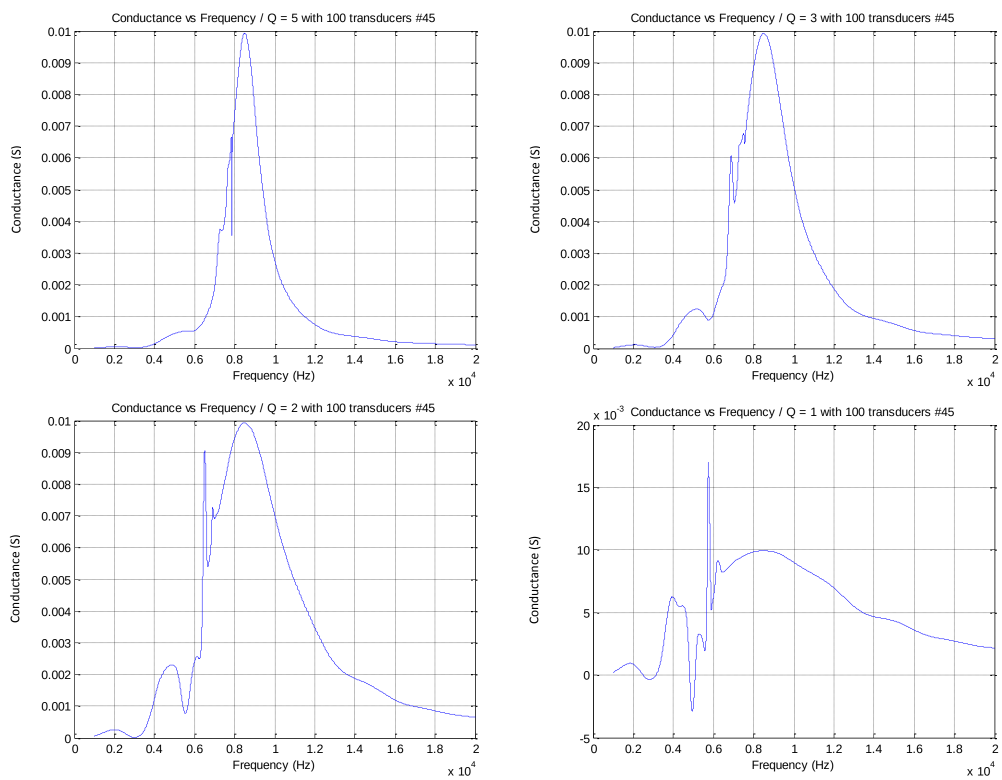

Figure C.1: Conductance vs Frequency of the corner (#45) element

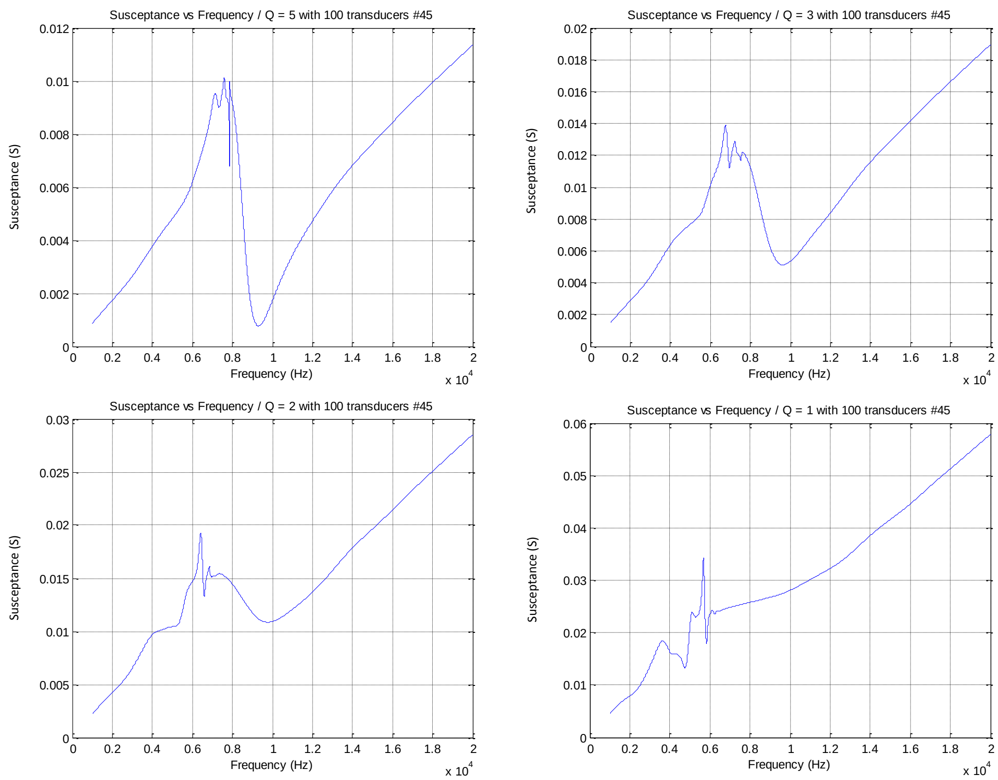

Figure C.2: Susceptance vs Frequency of the corner (#45) element

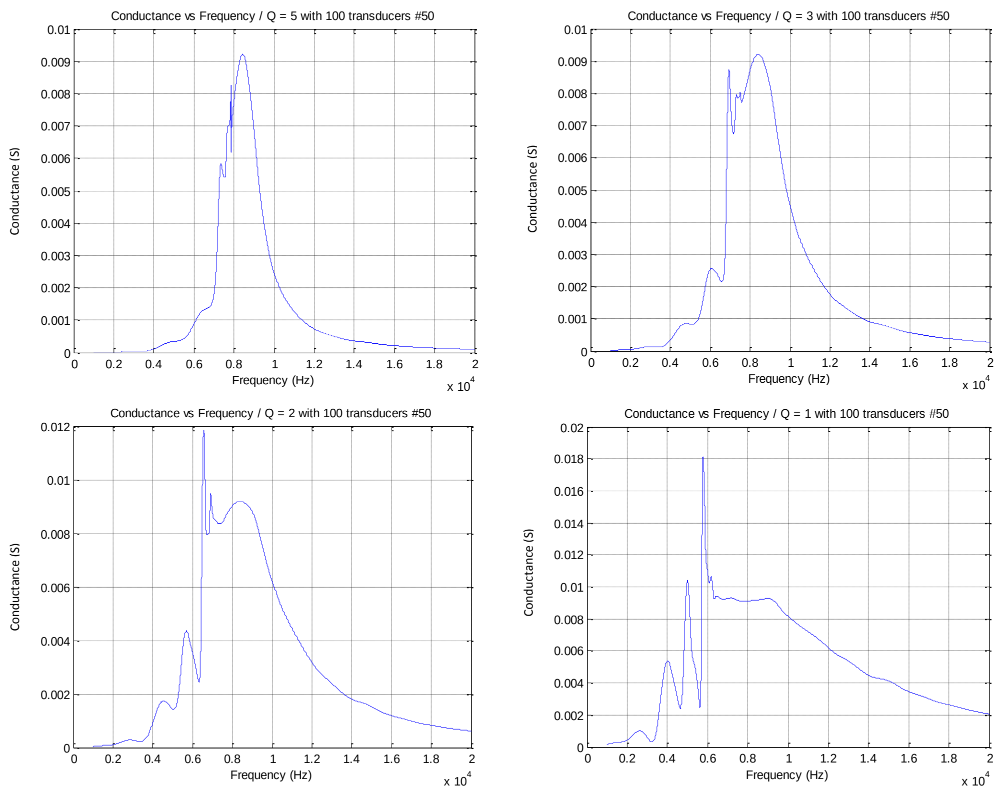

Figure C.3: Conductance vs Frequency of the corner (#50) element

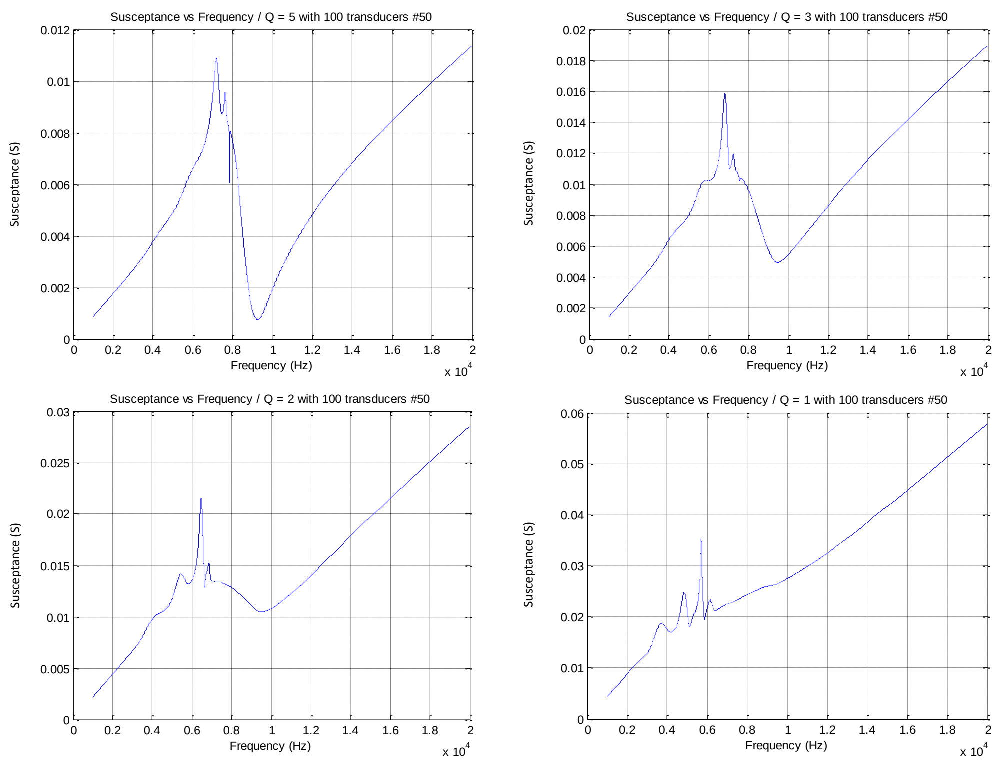

Figure C.4: Susceptance vs Frequency of the corner (#50) element

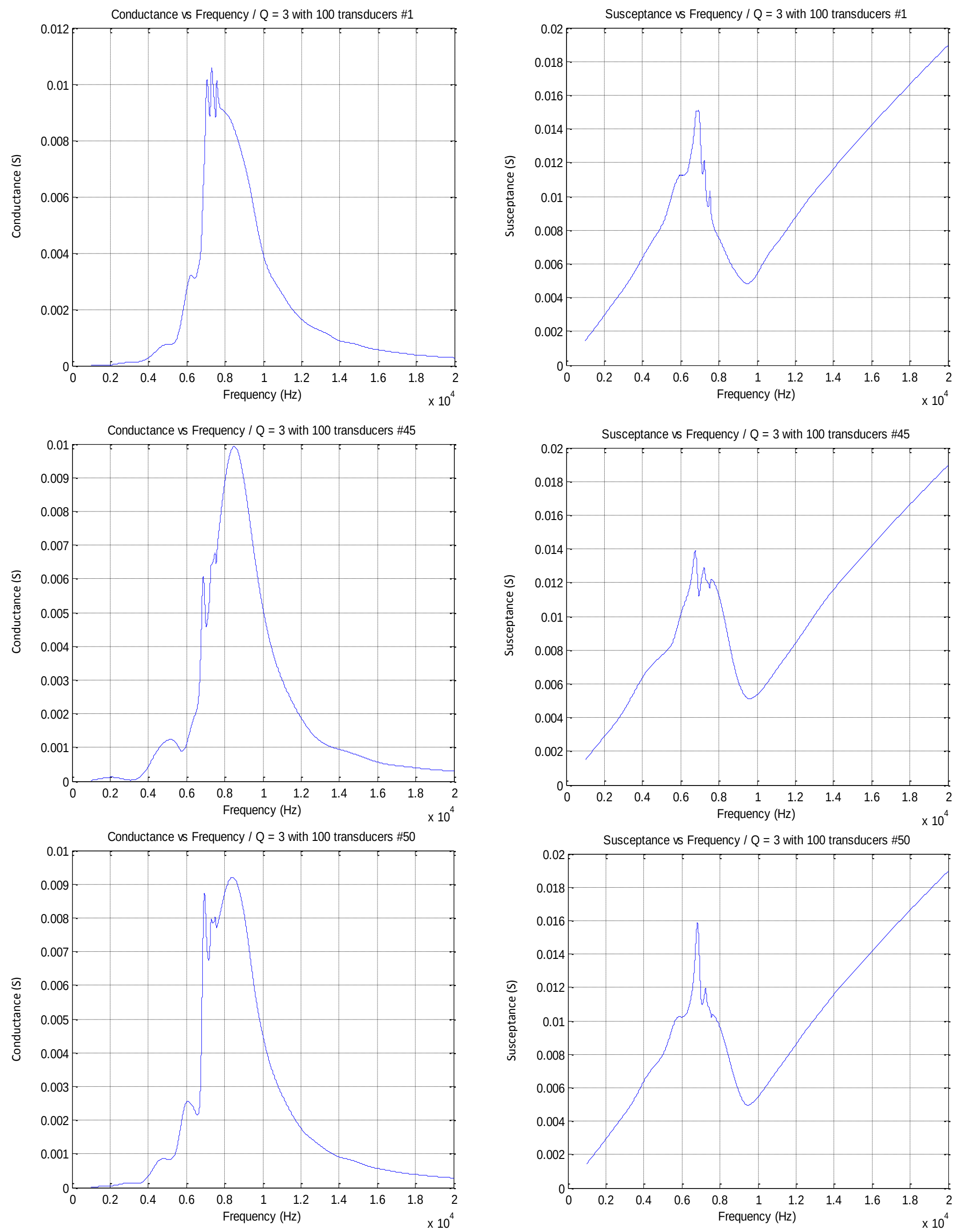

Figure C.5: Conductance/Susceptance vs Frequency of the corner (#1), center (#45) and edge (#50) elements with quality factor Q=3

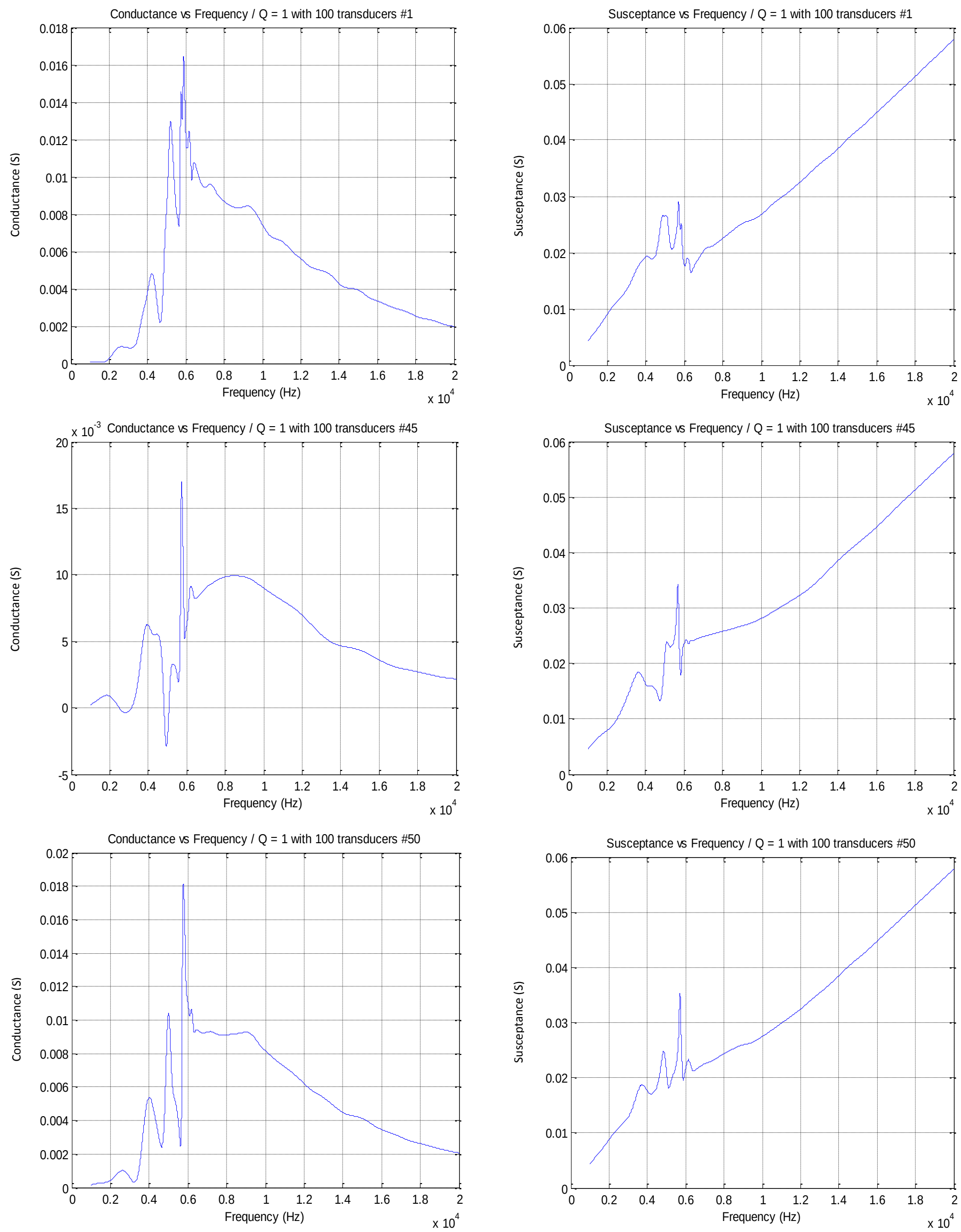

Figure C.6: Conductance/Susceptance vs Frequency of the corner (#1), center (#45) and edge (#50) elements with quality factor Q=1